Lu-Hf analyses of zircon from the Makoppa Dome and Amalia-Kraaipan area: 1 implications for evolution of the Kimberley and Pietersburg blocks of the Kaapvaal Craton.

Marlina A. Elburg, Marc Poujol

Lu-Hf analyses of zircon from the Makoppa Dome and Amalia-Kraaipan area: implications for evolution of the Kimberley and Pietersburg blocks of the Kaapvaal Craton.

Marlina A. Elburg[1], Marc Poujol[2]

1 Department of Geology, University of Johannesburg, South Africa; marlinae@uj.ac.za

2 Univ. Rennes, CNRS, Géosciences Rennes - UMR 6118, F-35000 Rennes, France; marc.poujol@univ-rennes1.fr

Abstract

Previously dated zircon crystals from the Amalia-Kraaipan granite-greenstone belts and Makoppa Dome were analysed for their Lu-Hf isotopic characteristics to refine the geological evolution of these areas. Samples from the Makoppa Dome, belonging to the Pietersburg Block, largely fall within the epsilon Hf-age range for granitoids from the eastern part of the block. However, the oldest 3.01-3.03 Ga trondhjemitic gneisses show that reworking of juvenile mafic crust started earlier in the western than the eastern part of the block, suggesting a diachronous tectonic evolution. The three granitoids from the Amalia-Kraaipan area fall within the field for Pietersburg and Kimberley block granitoids. Contribution from older crustal material is seen in a 3.08 Ga schist, likely derived from a volcanic protolith, from the Madibe Belt, in the far east of the Kimberley Block, with a mantle extraction age of 3.25-3.45 Ga. The data suggest that the Kimberley Block, like the Pietersburg Block, also contains (minor) ancient crustal components, derived from a depleted mantle source prior to 3.1 Ga. The new data suggest that the Kimberley and Pietersburg blocks underwent a very similar Paleo- to Mesoarchean crustal evolution, with a major crust formation event at 3.1-3.0 Ga followed by successive crust reworking until 2.77 Ga. Lavas of the Ventersdorp Supergroup, for which zircons from a ca. 2.75 lapilli tuff give εHf_i of +2, are the first evidence of a juvenile source, after 300 Myr of crustal reworking.

Introduction

The Kaapvaal Craton is one of the better-studied Archean cratons, thanks to its relatively accessible and well-exposed geological record. Its division into four separate terranes or blocks (Eglington and Armstrong, 2004), based on geochronological data, is now widely accepted (Figure 1), with the Swaziland Block having attracted the most academic attention as it hosts the craton's oldest rocks at 3.66-3.70 Ga (Compston and Kröner, 1988; Kröner et al., 1996; Robb et al., 2006; Zeh et al., 2011). Recorded ages are somewhat younger in the Witwatersrand and

Pietersburg blocks (Anhaeusser, 2019) at ≤3.34 Ga (Laurent and Zeh, 2015; Poujol and Anhaeusser, 2001). Because of its extensive cover, the Kimberley Block is the least known, and virtually no ages older than ca. 3.2 Ga have been found (Anhaeusser and Walraven, 1999; Cornell et al., 2018; Poujol et al., 2008). The boundaries between the four terranes are based on geophysically defined lineaments, which may or may not have any surface expression, as well as recognisable faults and shear zones, and extensions thereof (Eglington and Armstrong, 2004). As such, they are somewhat dependent on changing interpretations of the geophysical data (Corner and Durrheim, 2018), additional geochronological information and also geochemical data. In the latter respect, the development of the past fifteen years of laser ablation multi-collector inductively coupled mass spectrometry (LA-MC-ICPMS), which permits the determination of the Hf isotopic characteristics of the same zircon grains that provide the age of intrusions, needs to be mentioned. Zircon is the most robust carrier of U-Pb age data, and has therefore been the mineral of choice to obtain reliable geochronological information. Zircon's high contents of the element hafnium, a geochemical twin of zirconium, and limited amount of the radioactive parent element lutetium, makes them also the best carrier of Hf isotopic information. As mantle and crust have contrasting Lu/Hf ratios, they develop different Hf isotope ratios over time. Studying the Hf isotopic compositions of dated zircon crystals therefore allows us to test whether intrusions with the same age also have similar magma sources; and whether these sources were juvenile (mantle-derived), or incorporated older crustal materials. As isotopic information, unlike whole rock geochemistry, is only affected by the sources contributing to the magma, irrespective of crystal fractionation, it is a robust test for similarity among rocks of the same age. This technique has been applied successfully to a number of plutons of the Kaapvaal Craton (see overviews in Kröner et al., 2019 and Laurent et al., 2019, and the many works by Zeh and coworkers (e.g. 2009, 2011)), but a great number of intrusives of which the age is known has not been analysed for the Hf isotopic composition. In addition to providing information on the petrogenesis of the igneous rocks from which the zircon grains are derived, establishing an age-Hf isotopic zircon database for the Kaapvaal Craton is also important for the study of detrital zircon in sedimentary rocks, which provides information on the sediments' provenance.

To add to the available information on the geological evolution of the Kimberley and Pietersburg blocks and Kaapvaal Craton zircon age-Hf isotopic database, we performed Lu-Hf isotopic analyses on zircon samples of ten igneous rocks from the Amalia-Kraaipan area of the Kimberley Block and the Makoppa Dome of the Pietersburg Block that were analysed for their U-Pb characteristics previously (Anhaeusser and Poujol, 2004; Poujol et al., 2002; Poujol et al., 2008; Poujol et al., 2005). Our new data are compatible with the interpretation that the Makoppa Dome is indeed part of the Pietersburg Block, and provides the earliest evidence for reworking of juvenile mafic material in the region, whereas they add to our relatively poor knowledge of the Kimberley Craton. Additionally, these data are compared to the existing detrital zircon database for Archean-Paleoproterozoic Kaapvaal Craton and provide matches for zircon grains from the Witwatersrand Supergroup and Waterberg Group.

Geological background

The geology of the Pietersburg Block has mainly been studied in its eastern part, between the extension of the Palala Shear Zone and the Thabazimbi-Murchison Lineament (Figure 1c), which are interpreted to be the northern and southern boundary, respectively, of the Pietersburg Block (Eglington and Armstrong, 2004). The Southern Marginal Zone of the Limpopo Belt, which is located north of the Hout River Shear Zone (Figure 1c), is also deemed part of the Pietersburg Block (Eglington and Armstrong, 2004). The western part of the block, in which the Makoppa Dome is located, is separated from the eastern part by the ca. 2.05 Ga

Bushveld Complex, which straddles the boundary of the Witwatersrand and Pietersburg blocks. In its eastern part, the Pietersburg Block consists of ENE-WSW running greenstone belts (the Murchison, Giyani and Pietersburg belt), with several generations of granitoids. The oldest of these are the Goudplaats-Hout River tonalite-trondhjemite-granodiorite (TTG) gneisses at 3.2-3.43 Ga (Laurent and Zeh, 2015). Further TTG intrusions followed from 3.0 to ca. 2.8 Ga, and more K-rich magmatism from 2.9 to 2.67 Ga (see Laurent et al., 2019 for a review). Magmatism has been interpreted to reflect accretion of several arcs, and a >3.2 Ga continental nucleus, to the proto-Kaapvaal Craton, consisting of the Swaziland and Witwatersrand blocks. The Makoppa Dome straddles the boundary between South Africa and Botswana, with an area of ca. 7600 km^2. The only published work on the area is the paper by Anhaeusser and Poujol (2004), which also provides the ages of the zircon used for the present study. The rocks of the Makoppa Dome are largely obscured by post-Mesozoic sediments, but consist of both granitoids and greenstones (Figure 1b). The latter are amphibolites, serpentinite, talc/chlorite schists and banded iron formations. The granitoids, which were the focus of the U-Pb zircon and whole rock geochemistry study by Anhaeusser and Poujol (2004), are the Vaalpenskraal trondhjemite/tonalite gneiss, the Makoppa granodiorite/monzogranite and the Rooibokvlei granodiorite/monzogranite. Intrusion and deformation relationships define the Vaalpenskraal gneisses to be the oldest felsic rocks in the area.

The Kimberley Block of the Kaapvaal Craton has outcrops of Archean rocks only in the Kraaipan-Amalia area, and the area around Marydale. Granitoids from the latter area were recently subject of study by Cornell et al. (2018), who reported ages of ca. 2.95 to 2.72 Ga, and xenocrysts up to 3.18 Ga. This work also quotes unpublished ages up to 3.28 Ga from basement samples retrieved during diamond mining. This is similar to the ca. 3.25 Ga unpublished ages quoted by Drennan et al. (1990) for areas west of the Colesberg Lineament, which forms the boundary with the Witwatersrand Block. The Kraaipan area contains greenstone outcrops that occur as three discontinuous NNW-trending belts, the Stella, Kraaipan and Madibe belts, from W to E (Brandl et al., 2006). The greenstones of the Amalia area lie along the extension of the Stella Belt to the south (Figure 1a), and contain interbedded pyroclastic rocks; the discontinuous outcrops may represent tectonically juxtaposed slivers (Brandl et al., 2006). Granitoids, some containing greenstone remnants, occur in the Amalia and Kraaipan areas, but intrusive relationships are unclear because of poor exposures. The rocks of the Amalia area are overlain by Ventersdorp Supergroup Lavas, dated at 2729 ± 3 Ma (Poujol et al., 2005).

Sample description and ages

Table 1 gives an overview of the samples analysed. All background information, including cathodoluminescence images, can be found in the referenced papers.

Pietersburg Block

The five samples from the Makoppa Dome, in the western part of the Pietersburg Block, have been described by Anhaeusser and Poujol (2004), and the following is based on their findings. All samples have undergone some degree of sericitisation, but no other evidence of metamorphism was noted, apart from the gneissosity of the oldest samples.

Samples MK10 and MK11 were taken from the Vaalpenskraal trondhjemitic gneiss, along the Crocodile River in the north central part of the dome (Figure 1b). The zircon crystals are yellowish to pink in colour, elongated to prismatic, with some rounded edges. Cathodoluminescence imaging showed apparent core-rim structures, with brighter cores and darker rims; rare crystals showed simple igneous zoning. Dating of sample MK10 was done by LA-ICP-MS and yielded a weighted average $^{207}Pb/^{206}Pb$ age of 3013 ± 11 Ma, measured mostly on the bright cores. This was interpreted to represent the age of intrusion. Zircon rims gave a poorly constrained upper intercept age of ca. 2.6 Ga, interpreted to reflect a later metamorphic event.

Sample MK11 was also dated by LA-ICP-MS, but gave poor results with an older age, likely igneous, of 3034 ± 64 Ma, and a likely resetting event at 2842 ± 35 Ma.

Sample MK5 represents the Makoppa granodiorites/monzogranites and was taken near the town of the same name. These relatively large, yellow to amber crystals, showed simple zoning in CL imaging. Zircon crystals from this sample were analysed by ID-TIMS and define an upper intercept age of 2886 +3/-2 Ma, which was interpreted to reflect the intrusive age of this phase.

Samples MK2 and MK3 represent the Rooibokvlei granodiorite/monzogranites. MK2 yielded pink to metamict zircon grains, of which many showed complex zoning in CL imaging, but few crystals with simple igneous zoning were also present. ID-TIMS dating yielded an upper intercept age of 2777 ± 2 Ma. This was confirmed by LA-ICP-MS dating, which yielded an upper intercept age of 2777 ± 35 Ma. Many of the more complexly zoned crystals showed much younger ages, trending towards a lower intercept of ca. 800 Ma. Sample MK3 yielded crystals that were similar in character to those of MK2, and ID-TIMS dating gave an upper intercept age of 2797 ± 2 Ma. This is regarded as the emplacement age of this granitoid.

Kimberley Block

All five samples analysed come from the Kraaipan-Amalia area of the Kimberley Block. Three of them (Madibe1, MAD1 and KP5; Poujol et al., 2002; Poujol et al., 2008) come from the Kraaipan area (Figure 1c); these samples show limited sericitisation and epidotisation (Anhaeusser and Walraven, 1999). Two others (AL3, BOT1; Poujol et al., 2002; Poujol et al., 2005) come from near Amalia.

Sample Madibe-1 (Poujol et al., 2008) is a lower greenschist-facies quartz-sericite schist that has been interpreted, based on its whole rock geochemistry, as a calc-alkaline lava from the Madibe belt in the easternmost part of the Kraaipan area. The sample was taken in the hanging wall of the orebody of the Madibe gold mine. This borehole sample is located very close to the Colesberg Lineament (Figure 1c), which is interpreted to run through Mahikeng (McCarthy et al., 2018). Zircon crystals in this drill core sample were rare, but those present are euhedral and have well-defined oscillatory zoning. Eight concordant SIMS analyses yielded a weighted average $^{207}Pb/^{206}Pb$ emplacement age of 3083 ± 6 Ma, whereas one older xenocrystic grain gave a concordant $^{207}Pb/^{206}Pb$ date of 3201 ± 4 Ma.

Sample KP5 (Poujol et al., 2002), a pink granodiorite, was taken near the Kraaipan railway siding. Zircon crystals are prismatic, and show well-developed zoning in cathodoluminescence (CL) imaging. The ion microprobe analyses gave a weighted mean $^{207}Pb/^{206}Pb$ age of 2913 ± 17 Ma for the emplacement of this granodiorite, without any evidence of inheritance.

Sample MAD1 was taken near the town of Madibogo and consists of a grey granodiorite. Zircon grains look similar to those in KP5, and their ion microprobe emplacement age is also indistinguishable at 2917 ± 9 Ma. Some grains appear to have suffered Pb-loss with $^{207}Pb/^{206}Pb$ apparent ages down to 2629 ± 23 Ma.

Sample BOT1 was taken between Amalia and Schweizer-Reneke (Poujol et al., 2005) and consists of a little-deformed accretionary lapilli tuff, which still contains fresh volcanic glass (Jones and Anhaeusser, 1993). Two types of zircon crystals were extracted: prismatic, euhedral zircon with simple, CL-dark internal structures, and smaller, more rounded grains with a very bright CL-response. When analysed by ion microprobe, the latter type gave Mesoproterozoic dates (1038 ± 48 Ma and 1538 ± 50), and the former a weighted mean $^{207}Pb/^{206}Pb$ age of 2754 ± 5 Ma interpreted as the emplacement age.

Sample AL3 (Poujol et al., 2002) was taken to the SSE of Amalia and represents a fine-grained leuco-trondhjemite gneiss, interpreted to be representative of the earliest basement in this area. Zircon crystals are euhedral to subhedral, pink, and CL imaging shows zoning and potential core-rim structure. Ion microprobe analyses, however, show a largely homogeneous age group with a weighted mean $^{207}Pb/^{206}Pb$ emplacement age of 2939 ± 10 Ma, although Pb-loss towards a lower intercept around 1.25 Ga was also observed. Only one core gave a near-concordant $^{207}Pb/^{206}Pb$ apparent age of 3178 ± 10 Ma.

More detailed descriptions of the samples, as well as CL images of the zircon crystals, are given in the cited publications.

Analytical techniques

LA-MC-ICPMS analyses for Lu-Hf were done on the same mounts that were imaged in the course of the geochronological investigations. The images and age results were used as a guide for the ablations, but not all zircon grains used for the study had been analysed for their U-Pb isotopic characteristics. The $^{207}Pb/^{206}Pb$ ages quoted in the previous section were used for the calculation of initial isotope ratios. The Lu-Hf analyses were done at the Department of Geology, University of Johannesburg, using a NPII MC-ICP-MS and ASI Resolution laser ablation system. The spot size used was 50-70 µm, and ablations were done at a repetition rate of 6-7 Hz; these parameters were adjusted to match the size and expected depth of the domain to be ablated. The fluence was ca. 4.6 J/cm^2. For details on the data reduction, including interference corrections, see Jacobs et al. (2017). Reference materials analysed during the course of the study gave results within uncertainty (quoted at the 2 sigma level) of published values for $^{176}Hf/^{177}Hf$ (Mud Tank: 0.282495 ± 0.000018, n=16; TEM-2: 0.282658 ± 0.000034, n=13; LV11: 282814 ±0.000016, n= 8). Additionally, the quality of the analyses for the unknowns was monitored by measuring their invariant $^{178}Hf/^{177}Hf$ and $^{174}Hf/^{177}Hf$ ratios, which yielded averages of 1.467277 ± 0.000053 and 0.008661 ± 0.000060, respectively. All results can be found in Electronic Supplement 1.

The measured $^{176}Hf/^{177}Hf$ ratios for the unknowns were calculated to their initial value using the measured $^{176}Lu/^{177}Hf$ ratios, a ^{176}Lu decay constant of $1.867*10^{-11}$ year^{-1} (Scherer et al., 2007) and the emplacement ages obtained during previous studies

(Table 1). The calculations of epsilon Hf were done with a present-day chondritic $^{176}Hf/^{177}Hf$ value of 0.282785 and $^{176}Lu/^{177}Hf$ of 0.0336 (Bouvier et al., 2008). Depleted mantle parameters are $^{176}Hf/^{177}Hf$ 0.28325 and $^{176}Lu/^{177}Hf$ of 0.0388, following Griffin et al. (2000).

Results

Full results can be found in Electronic Supplement 1; averages are given in Table 1.

Pietersburg Block

For trondhjemitic gneiss sample MK10, twelve ablations were performed, with two targeting younger rims. The ten analyses on the igneous cores gave $^{176}Hf/^{177}Hf_{3013}$ 0.28094-0.28099 (Figure 2a), corresponding to a εHf_{3013} of +3.5 to +5.5 (Figure 2b), with an average (mean) of +4.1 ± 1.2 (2 standard deviations). The two younger rims gave only marginally higher initial Hf isotope ratios.

Ten zircon grains were analysed for the other sample of trondhjemitic gneiss, MK11, from the same area, and the results are consistent with the other sample, giving an average εHf_{3034} of 4.9 ± 1.3.

Sample MK5 from the Makoppa monzogranite is represented by ten analyses. $^{176}Hf/^{177}Hf_{2886}$ varies from 0.28093 to 0.28101, corresponding to εHf_{2886} of 0 to +3.0, with an average of +1.6 ± 1.9.

Twelve zircon crystals were analysed for the MK3 Rooibokvlei monzogranite. These give $^{176}Hf/^{177}Hf_{2797}$ 0.28095-0.28105, or εHf_{27976} -1.2 to +2.2, and an average εHf_{2797} +0.1 ± 2.

Ten analyses were done on the other Rooibokvlei monzogranite sample, MK2, of which the eight analyses with igneous ages gave results indistinguishable from sample MK3, with average εHf_{2777} -0.4 ± 1.5. The two areas with younger $^{207}Pb/^{206}Pb$ apparent ages are indistinguishable in their initial $^{176}Hf/^{177}Hf$ ratios from the older grains.

Kimberley Block

For quartz-sericite schist sample Madibe-1, fourteen zircon crystals were analysed, with one spot per zircon. This also included the one older zircon xenocryst at 3.2 Ga. Excluding the latter, 12 grains gave initial $^{176}Hf/^{177}Hf$ values of 0.28077 to 0.28089, which translates into epsilon-Hf_{3083} values of -0.8 to +3 (Figure 2a,b). The one dated older zircon gave a lower $^{176}Hf/^{177}Hf_{3201}$ of 0.280728, corresponding to εHf_{3201} = +0.4. One of the undated grains gave a similarly low value, and could therefore also represent an older grain. The average of the 12 zircon grains is εHf_{3083} +1.2 ± 3 (2SD).

For granodiorite sample KP5, eleven analyses were performed, giving $^{176}Hf/^{177}Hf_{2913}$ from 0.28096 to 0.28100, and a range of εHf_{2913} of +1.8 - +4.5. The average is εHf_{2913} of +2.8 ± 1.5.

Fourteen analyses were done on zircon from granodiorite sample MAD1, including two analyses on a single grain, of which the rim had given a younger age. Excluding this grain, twelve analyses gave $^{176}Hf/^{177}Hf_{2917}$ from 0.28092 to 0.28099, or εHf_{2917} of +0.6 - +3.0, resulting in an average εHf_{2917} of +2.8 ± 1.5, which is indistinguishable from the previous sample. For the grain that had given a ca. 2.63 Ga rim age, both core and rim gave somewhat lower initial Hf isotopic values, indicating that there might have been some overlap between the two domains during the analyses.

For accretionary lapilli tuff sample BOT1 from the Amalia area, thirteen zircon crystals were analysed. Ten of these constitute a homogeneous group, with $^{176}Hf/^{177}Hf_{2754}$ 0.28106-0.28110, or εHf_{2754} of +1.6 - +3.2, with average εHf_{2754} of +2.3 ± 1.0. Three undated grains gave much higher $^{176}Hf/^{177}Hf$ ratios (0.2817-0.2824) and are assumed to be part of the Mesoproterozoic population (ca. 1-1.5 Ga) described by Poujol et al. (2005). As these analyses cannot give any information on the

Archean evolution of the Kaapvaal Craton, which is the subject of this paper, they will not be discussed further.

Sixteen grains were analysed from leuco-trondhjemite sample AL3. Thirteen of these cluster at ^{176}Hf/^{177}Hf$_{2939}$ 0.28096-0.28101, corresponding tor εHf$_{2939}$ of +2.4 - +4.4, with an average of +3.2 ± 1. The one older xenocryst gave significantly lower ^{176}Hf/^{177}Hf$_{3178}$ of 0.28087 (εHf$_{3178}$ = +5). Two undated grains also give substantially lower ^{176}Hf/^{177}Hf than the main group (0.28084), so zircon grains with older ages could potentially be more common in sample AL3 than detected by Poujol et al. (2002).

Discussion

To facilitate the interpretation of the data, the average epsilon Hf values for the ten analysed samples are shown in Figure 3a, together with similarly averaged literature data. The two older xenocrystic cores are shown separately. In this diagram, all other Kimberley Block Hf isotopic data points are from Cornell et al. (2018), whereas the Pietersburg Block data are those used in the recent review paper by Laurent et al. (2019). All references to the literature data are given in Electronic Supplement 2.

Pietersburg Block

The general geochemistry and ages of the granitoids of the Makoppa Dome in the Pietersburg Block were found to be similar to the data from the area to the east of the Bushveld Complex (Laurent et al., 2019). Our new zircon Hf isotope data confirm this finding for the ca. 2.9-2.8 Ga samples from the Rooibokvlei (MK2, 3) and Makoppa (MK5) granodiorite/monzogranite. These three samples overlap in terms of age and Hf isotopic composition with the various biotite-(muscovite) granites from the eastern part of the Pietersburg Block. The two samples from the Vaalpenskraal trondhjemitic gneisses are, however, slightly different. Apart from three samples of tonalite-trondhjemite-granodiorite (TTG) of 3.35-3.25 Ga that have been interpreted to form the nucleus of a separate ‘crustal nucleus’ (Laurent et al., 2019), the Vaalpenskraal trondhjemite is the oldest TTG in the Pietersburg Block of which Hf isotope data have been obtained. The samples are slightly older than the ca. 2.97 Free State Tonalite of the Rooiwater Complex and Rubbervale felsic volcanics, both in the Murchison Belt, for which the strongly superchondritic data were reported by Zeh et al. (2013). Similarly, the Vaalpenskraal trondhjemitic gneisses also record initial epsilon $Hf_{3.0Ga}$ values of +4 - +5. These age-epsilon Hf values overlap with a single older zircon reported in a 2.88 Ga trondhjemite sampled just north of the Rooiwater Complex by Laurent and Zeh (2015). A slightly older zircon xenocryst (at 3.115 Ga) with an even higher initial epsilon Hf value (+6) was reported by the same authors from a 2.83 Ga biotite granite north of the Hout River Shear zone.

The trend in the linear age-epsilon Hf array for the eastern part of the Pietersburg Block has been interpreted by Laurent and Zeh (2015) and Laurent et al. (2019) as reflecting partial melting of depleted mantle at 3.15-2.97 Ga, followed by reworking of the mafic rocks to TTGs at 2.97-2.88 Ga. Subsequently, the TTG-type crust with a $_{176}$Lu/$_{177}$Hf ratio of 0.0022 was internally further transformed into grey gneisses and biotite-granites, with only very minor contributions from older crust. Our new data from the Makoppa Dome show that formation of felsic crust (Vaalpenskraal trondhjemite, with SiO_2 contents of 69-75%, Anhaeusser and Poujol, 2004) already started 3.03-3.01 Ga ago. Assuming a mafic protolith with $_{176}$Lu/$_{177}$Hf=0.022, the Hf isotope data give a mantle extraction age of 3.15-3.10 Ga (Figure 3a, Table 1), in agreement with the estimate by Laurent et al. (2019). The three samples from the two younger granitoids fall within the $_{176}$Lu/$_{177}$Hf=0.0022 array that envelops the Pietersburg Block intrusives from the eastern side. All five samples fall towards the lower part of the array, in agreement with the old mantle extraction age of the earliest samples compared to those from the eastern side of the block. Note that none of the samples fall below the array, which would reflect a contribution of older continental crust (Figure 3a). This is in agreement with their distal position relative to the old continental nucleus on the eastern side, and the lack of older inherited zircon.

The average $^{176}Lu/^{177}Hf$ ratio of the zircon crystals is plotted in Figure 3b (in contrast to the previously discussed $^{176}Lu/^{177}Hf$ ratios of the protoliths that define the arrays), showing that our samples also plot in the same field as previously analysed zircon grains from the Pietersburg Block. The two younger samples, of the Rooibokvlei monzogranite have higher $^{176}Lu/^{177}Hf$ than the other three samples, which matches their whole rock composition, with Lu concentrations 3-8 times higher in the Rooibokvlei samples (Anhaeusser and Poujol, 2004). This adds to recent discussions whether zircon trace element data can be used to determine the composition of the magma it crystallised from (e.g. Chapman et al., 2016; Reimink et al., 2020). In this case, this appears to hold, on the assumption that the whole rock compositions are representative for the liquid composition.

Although a connection between the Murchison Belt Free State Tonalite + Rubbervale Volcanics and the Vaalpenskraal Trondhjemite seemed possible based on the age and Hf isotopic characteristics of the zircons, the zircon $^{176}Lu/^{177}Hf$ ratios (Fig. 3b) are much higher for the three Murchison Belt samples than for the Makoppa Dome samples. This is a reflection of the whole rock geochemistry, with flat normalised REE patterns for the Rubbervale Volcanics (Schwarz-Schampera et al., 2010), and steeply downward sloping patterns for the Vaalpenskraal Trondhjemite (Anhaeusser and Poujol, 2004). It therefore seems that the Makoppa Dome samples reflect crustal reworking, which must have taken place very shortly after juvenile crust formation, based on the Hf isotopic signature. The Murchison Belt samples, on the other hand, are evidence of juvenile crust formation, rather than reworking.

Kimberley Block

Sample AL3, a fine-grained trondhjemitic dyke from the Amalia area has an age that is ca. 20 Ma older than the two more K-rich granitoids from the Kraaipan area, MAD1 and KP5, but the three samples are indistinguishable in terms of $^{176}Hf/^{177}Hf$ and $^{176}Lu/^{177}Hf$ (Figure 3a,b). They fall within the same array as the Pietersburg Block intrusives, with epsilon Hf values of +1 to +2 at ca. 2.9 Ga, and also overlap with some of the granitoids from the Marydale area described by Cornell et al. (2018). The one older zircon in sample AL3, at ca. 3.18 Ga, falls slightly off the array for the Pietersburg Block. It plots very close to the depleted mantle line, and therefore gives a mantle extraction age of ca. 3.2 Ga, assuming a mafic protolith.

Schist sample Madibe-1, presumably a metamorphosed volcanic rock, has an igneous age of ca. 3.08 Ga, and lies completely off the Pietersburg array, with an initial epsilon Hf value just above 0. If this isotopic signature reflects reworking of mafic crust with $^{176}Lu/^{177}Hf$ 0.022, then the mantle extraction age is ca. 3.43 Ga (Table 1); this age would fit with 3.43 Ga zircon found in a volcano-sedimentary sample from the same area (Poujol et al., 2008). However, if this is part of a TTG array, with $^{176}Lu/^{177}Hf$ 0.0022, then mantle extraction would be around 3.25 Ga. Here, it must be noted that the scatter of Hf isotope data for this sample is larger than for the other samples analysed in this study (Fig. 2a), and the data show a rough negative correlation between $^{176}Lu/^{177}Hf$ ratio and initial $^{176}Hf/^{177}Hf$ ratio (not shown). As zircons can take up HREE during alteration processes (Pidgeon et al., 2019), it is possible that the spread towards lower $^{176}Hf/^{177}Hf$ ratios is related to this effect. In that case, the mantle extraction ages quoted here are over-estimates. Either way, the one older grain of 3.2 Ga that was analysed for its Hf isotopic composition actually has a $^{176}Hf/^{177}Hf$ ratio that is lower than that of the main population, which is the opposite of what would be expected if this zircon had been derived from 3.45-3.25 Ga juvenile crust that was the protolith to the Madibe-1 lava. As such, the one older zircon plots close to the data for the Pietersburg ‘old continental nucleus’ of the Goudplaats-Hout River gneiss, although a single older zircon may be of limited significance. The main zircon population of sample Madibe-1 shows most similarity in terms of its Hf isotopic composition and Lu/Hf ratio to samples from the adjacent Witwatersrand Block (Figure 3a,b), such as the granites studied by Frimmel et al. (2009) from a borehole west of Carletonville. Considering that this is only a single sample, it is hard to say whether this can be interpreted as the Madibe greenstone area having a greater affinity to the Witwatersrand than the Kimberley Block, but, considering its location so close to the Colesberg Lineament, this possibility cannot be excluded.

Sample BOT1 also plots away from the other Kimberley Block samples, but now on the young, higher-epsilon Hf side. It shows some similarities in its Hf isotopic composition to the slightly older Pietersburg Block biotite granite samples GH-2 and GHBR-2 analysed by Laurent and Zeh (2015). Its signature is however significantly different from similarly aged granitoids from the Marydale area analysed by Cornell et al. (2018). The 2.75 Ga age of lapilli tuff sample BOT1, interpreted to be part of the greenstone basement, was discussed at length by Poujol et al. (2005), since it appears rather young for the age of the greenstone succession in the area, especially in the light of the ages of the granitoids of 2.8-3.0 Ga. Some granitoids in the Marydale area of the Kimberley Block have provided similar ages, which Cornell et al. (2018) related to crustal melting in connection with plume activity of the Ventersdorp Supergroup lavas. Although the Ventersdorp volcanism was long assumed to have started at ca. 2.71 Ga (Armstrong et al., 1991), more recent work has shown activity at 2791-2779 (Klipriviersberg Group), 2754–2709 (Platberg Group) and 2709–2683 Ma (Allanridge Group) (Gumsley et al., 2020). Indeed, a felsic porphyry sample from the Platberg Group of the Ventersdorp Supergroup in the Amalia area was dated at 2729 ± 3 Ma (U-Pb zircon SHRIMP upper intercept age) by Poujol et al. (2005). This porphyry was interpreted to overlie the granite-greenstone succession. It is therefore likely that the lapilli tuffs from which sample BOT1 was derived are also part of the Ventersdorp Supergroup, rather than the greenstone basement. This ties in with the work by de Kock et al. (2012), who sampled accretionary lapilli-bearing tuffs near Taung, 50 km to the SW of sample BOT-1, of the Mohle Formation, which is a local correlative of the Kameeldoorns Formation of the Platberg Group of the Ventersdorp Supergroup. Zircons from these tuffs gave a concordia age of 2735 ± 3 Ma. Although no Hf isotope data are available for the Ventersdorp Supergroup, the Nd isotopic characteristics for the Platberg Group appear to be subchondritic (see Humbert et al., 2019 for an overview of the existing isotope data), which does not agree with the decidedly superchondritic Hf isotope values of the zircon grains of BOT1. Although the Klipriviersberg Group might provide a match with marginally superchondritic Nd isotope values, the age of 2754 ± 5 Ma for BOT1 appears to preclude this. More information on the isotopic composition of the Ventersdorp Supergroup is therefore needed to resolve this matter further. It is, however, the first evidence of tapping of a juvenile source after ca. 300 Myr of crustal reworking in the area.

Comparison to detrital zircon data

In as far as our new data overlaps with previously published analyses for granitoids from the Kaapvaal Craton, they only broaden the choice of provenance areas for detrital zircon data. However, our data for the Makoppa Vaalpenskraal trondhjemite and Amalia lapilli tuff have quite a distinct age-epsilon Hf signature, and can therefore provide a possible match for detrital zircon grains of which the protosource has remained elusive.

As Figure 4 shows, our three ‘uncommon’ samples (BOT-1, MK10, MK11) only show limited overlap with published detrital zircon data (see Electronic Supplement 2 for full references of literature data) from Archean successions, the Magaliesberg Formation from the Paleoproterozoic Pretoria Group or the Waterberg Group. However, some overlap is noted between the Vaalpenskraal trondhjemite samples MK10 and 11 and detrital zircon from the Eldorado Reef in the upper part of the

Witwatersrand Supergroup (Koglin et al., 2010). This is in agreement with paleocurrent direction from the north and west (Frimmel et al., 2009), and the connection between the Pietersburg and Witwatersrand blocks (Zeh et al., 2013; Laurent et al., 2019) around the time of deposition of the upper Witwatersrand Supergroup at 2.9-2.78 Ga. The characteristics of the accretionary lapilli tuff from the Amalia area provide a match for zircon from the Svaershoek Formation of the Waterberg Group (Andersen et al., 2019). It is however doubtful that this equates to direct derivation of the sediment from these outcrops, considering the depositional age of ca. 2.05 Ga for the Svaershoek Formation, which is 700 Ma younger than the Amalia lapilli tuff. This time gap would leave sufficient time for several cycles of erosion and redeposition to take place. Moreover, if this lapilli tuff indeed belongs to the Ventersdorp Supergroup rather than the greenstone basement, the potential protosource area would have had a large areal extent; and, within analytical uncertainty, the zircon grains from the Waterberg Group also overlap with granitoids from the Pietersburg Block, so this derivation is ambiguous.

Conclusions regarding the evolution of the Kaapvaal Craton

Our new data show that the Makoppa Dome is indeed part of the Pietersburg Block, despite being separated from the eastern granitoids by the Bushveld Complex, which itself is obscured by the Paleoproterozoic sedimentary rocks of the Waterberg Group. The Makoppa Dome samples also provide the first Hf-in-zircon evidence that reworking of juvenile mafic material started as early as 3.01-3.03 Ga, immediately after formation of the mafic crust from a depleted mantle source. This is ca. 50 million years younger than what is known for the eastern Pietersburg Block (Laurent and Zeh, 2015; Zeh et al., 2013), where the TTGs of the Groot Letaba-Duivelskloof Domain provide the first evidence for this. This could mean that the tectonic scenario sketched in Laurent et al. (2019) is actually diachronous, with an earlier onset of events on the western side of the Pietersburg Block.

The data from the three granitoids of the Amalia-Kraaipan area of the Kimberley block fall within the same epsilon-Hf – age space as Pietersburg granitoids – as do the granitoids from the Marydale area analysed by Cornell et al. (2018). Therefore, the Hf isotopic evolution of the two blocks is starting to look remarkably similar, including evidence for the involvement of older crust (at least as old as 3.2 Ga, based on near-concordant analyses of older zircon). The schist sample from the Madibe area could potentially bear evidence of this older crust – although its igneous age is ca. 3.08 Ga, the Hf isotopic composition of the zircon necessitates a mantle extraction age of 3.25-3.43 Ga, depending on the assumed protolith. However, another possibility is that the area, which is very close to the Colesberg Lineament, bears a closer resemblance to the Witwatersrand Block, for which an older crustal history is more evident than for either the Kimberley or Pietersburg Block. The previously reported ca. 2.75 age for a lapilli tuff in the Amalia Belt (Poujol et al., 2005), which was interpreted as reflecting the age of the greenstone belt, likely reflects magmatism associated with the Ventersdorp Supergroup, although the Hf isotopic signature of the latter is not known, so direct comparisons cannot be made.

Acknowledgements:

The LA-MC-ICPMS laboratory is funded by NRF-NEP grant #93208, and is supported by DSI-NRF CIMERA, of which the support is gratefully acknowledged. Henriette Ueckermann is thanked for her help with the analyses. MAE acknowledges funding from NRF IFRR grant #119297, as well as from DSI-NRF CIMERA for this work. The paper benefitted from constructive reviews by Armin Zeh, Elis Hoffmann and Hugh Rollinson.

Figure captions:

Figure 1: Overview location map (a), showing boundaries between the blocks after Eglington and Armstrong (2004); locations for the samples from the Makoppa Dome (after Anhaeusser and Poujol, 2004) in the Pietersburg Block (b) and from the Kraaipan-Amalia area (after Poujol et al., 2002) of the Kimberley Block (c). The white areas in panel (c) are mainly lavas of the Ventersdorp Supergroup. HRSZ = Hout River Shear Zone; TML: Thabazimbi-Murchison Lineament; PSZ = Palala Shear Zone; CL= Colesberg Lineament

Figure 2: Obtained Hf isotope data for the Amalia-Kraaipan (triangles) and Makoppa Dome (squares) samples in initial $^{176}Hf/^{177}Hf$ (a) and epsilon Hf (b) versus age space. All data are calculated for the time of igneous zircon crystallization. The inset shows the data including the younger Archean zircon domains, interpreted to reflect later reworking or Pb-loss. The typical uncertainties (2 SD) are based on multiple analyses of reference materials.

Figure 3: a. Average εHf_i versus age for the samples from this study (large symbols), together with pluton-averages for published analyses, plus single analyses for inherited (older) zircon grains within the granitoids (references in Electronic Supplement 2). Trendlines for mafic crust ($^{176}Lu/^{177}Hf$ = 0.022) and typical TTG ($^{176}Lu/^{177}Hf$ = 0.0022) are also shown. The depleted mantle line is following Griffin et al. (2000). Note that tuff sample BOT1 is more primitive than any other sample, and likely represents volcanism associated with the Ventersdorp Supergroup. See text for further discussion.

b. Zircon $^{176}Lu/^{177}Hf$ (pluton averages) versus age for the same samples as in a. Note that the zircons from the Rubbervale Volcanics and Free State Tonalite from the Murchison Belt (Zeh et al., 2013) have much higher $^{176}Lu/^{177}Hf$ than the Makoppa Dome samples, despite their ages and Hf isotopic compositions being similar. The former are evidence of juvenile crust formation, whereas the latter, together with slightly younger samples of the Groot Letaba-Duivelskloof (GLD) TTGs (Laurent and Zeh, 2015) are a result of crustal reworking.

Figure 4: As Figure 3a, but with the addition of detrital zircon data from Archean successions, Waterberg Group and Magaliesberg Formation (see Electronic Supplement 2 for references). Our new Hf isotope data widen the possible provenance areas for Archean sedimentary rocks, and could explain some of the yet unmatched grains in the Eldorado Reef of the Witwatersrand Supergroup and Waterberg Group.

References:

Andersen, T., Elburg, M.A. and Van Niekerk, H.S., 2019. Detrital zircon in sandstones from the Palaeoproterozoic Waterberg and Nylstroom basins, South Africa: Provenance and recycling. South African Journal of Geology, 122, 79-96.

Anhaeusser, C.R., 2019. Palaeo- Meso- and Neoarchaean Granite-Greenstone Basement Geology and Related Rocks of the Central and Western Kaapvaal Craton, South Africa, in: Kröner, A. and Hofmann, A. (Eds.), The Archaean geology of the Kaapvaal Craton, southern Africa. Springer, 55-81.

Anhaeusser, C.R. and Poujol, M., 2004. Petrological, geochemical and U-Pb isotopic studies of Archaean granitoid rocks of the Makoppa Dome, northwest Limpopo Province, South Africa. South African Journal of Geology, 107, 521-544.

Anhaeusser, C.R. and Walraven, F., 1999. Episodic granitoid emplacement in the western Kaapvaal Craton: evidence from the Archæan Kraaipan granite-greenstone terrane, South Africa. Journal of African Earth Sciences, 28, 289-309.

Armstrong, R.A., Compston, W., Retief, E.A., Williams, I.A. and Welke, H.J., 1991. Zircon ion microprobe studies bearing on the age and evolution of the Witwatersrand triad. Precambrian Research, 53, 243-266.

Brandl, G., Cloete, M. and Anhaeusser, C.R., 2006. Archaean greenstone belts, in: Johnson, M.R., Anhaeusser, C.R.and Thomas, R.J. (Eds.), The Geology of South Africa. Geological Society of South Africa, Johannesburg/Council for Geosciences, Pretoria, pp. 9-56.

Bouvier, A., Vervoort, J.D. and Patchett, P.J., 2008. The Lu-Hf and Sm-Nd isotopic composition of CHUR: Constraints from unequilibrated chondrites and implications for the bulk composition of terrestrial planets. Earth and Planetary Science Letters, 273, 48-57.

Chapman, J.B., Gehrels, G.E., Ducea, M.N., Giesler, N. and Pullen, A., 2016. A new method for estimating parent rock trace element concentrations from zircon. Chemical Geology, 439, 59-70.

Compston, W., Kröner, A., 1988. Multiple zircon growth within early Archaean tonalitic gneiss from the Ancient Gneiss Complex, Swaziland. Earth and Planetary Science Letters, 87, 13-28.

Cornell, D.H., Minnaar, H., Frei, D. and Kristoffersen, M., 2018. Precise microbeam dating defines three Archaean granitoid suites at the southwestern margin of the Kaapvaal Craton. Precambrian Research, 304, 21-38.

Corner, B. and Durrheim, R.J., 2018. An Integrated Geophysical and Geological Interpretation of the Southern African Lithosphere, in: Siegesmund, S., Basei, M.A.S., Oyhantçabal, P. and Oriolo, S. (Eds.), Geology of Southwest Gondwana. Springer, pp. 19-62.

de Kock, M.O., Beukes, N.J. and Armstrong, R.A., 2012. New SHRIMP U–Pb zircon ages from the Hartswater Group, South Africa: Implications for correlations of the Neoarchean Ventersdorp Supergroup on the Kaapvaal craton and with the

Fortescue Group on the Pilbara craton. Precambrian Research, 204-205, 66-74.

Drennan, G.R., Robb, L.J., Meyer, F.M., Armstrong, R.A. and de Bruiyn, H., 1990. The nature of the Archaean basement in the hinterland of the Witwatersrand Basin: II. A crustal profile west of the Welkom Goldfield and comparisons with the Vredefort crustal profile. South African Journal of Geology, 93, 41-53.

Eglington, B.M. and Armstrong, R.A., 2004. The Kaapvaal Craton and adjacent orogens, southern Africa: a geochronological database and overview of the geological development of the craton. South African Journal of Geology, 107, 13-32.

Frimmel, H.E., Zeh, A., Lehrmann, B., Hallbauer, D. and Frank, W., 2009. Geochemical and Geochronological Constraints on the Nature of the Immediate Basement next to the Mesoarchaean Auriferous Witwatersrand Basin, South Africa. Journal of Petrology, 50, 2187-2220.

Griffin, W.L., Pearson, N.J., Belousova, E., Jackson, S.E., van Achterbergh, E., O'Reilly, S.Y., Shee, S.R., 2000. The Hf isotope composition of cratonic mantle: LAM-MC-ICPMS analysis of zircon megacrysts in kimberlites. Geochimica et Cosmochimica Acta, 64, 133-147.

Gumsley, A., Stamsnijder, J., Larsson, E., Söderlund, U., Naeraa, T., de Kock, M., Sałacińska, A., Gawęda, A., Humbert, F. and Ernst, R., 2020. Neoarchean large igneous provinces on the Kaapvaal Craton in southern Africa re-define the formation of the Ventersdorp Supergroup and its temporal equivalents. GSA Bulletin.

Humbert, F., de Kock, M., Lenhardt, N. and Altermann, W., 2019. Neoarchaean to Early Palaeoproterozoic Within-Plate Volcanism of the Kaapvaal Craton: Comparing the Ventersdorp Supergroup and the Ongeluk and Hekpoort Formations (Transvaal Supergroup), in: Kröner, A. and Hofmann, A. (Eds.), The Archaean Geology of the Kaapvaal Craton, Southern Africa. Springer, 277-302.

Jacobs, J., Opås, B., Elburg, M.A., Läufer, A., Estrada, S., Ksienzyk, A.K., Damaske, D. and Hofmann, M., 2017. Cryptic sub-ice geology revealed by a U-Pb zircon study of glacial till in Dronning Maud Land, East Antarctica. Precambrian Research, 294, 1-14.

Jones, I.M. and Anhaeusser, C.R., 1993. Accretionary lapilli associated with Archaean banded iron formations of the Kraaipan Group, Amalia greenstone belt, South Africa. Precambrian Research, 61, 117-136.

Koglin, N., Zeh, A., Frimmel, H.E. and Gerdes, A., 2010. New constraints on the auriferous Witwatersrand sediment provenance from combined detrital zircon U–Pb and Lu–Hf isotope data for the Eldorado Reef (Central Rand Group, South Africa). Precambrian Research, 183, 817-824.

Kröner, A., Hegner, E., Wendt, J.I. and Byerly, G.R., 1996. The oldest part of the Barberton granitoid-greenstone terrain, South Africa: evidence for crust formation between 3.5 and 3.7 Ga. Precambrian Research, 78, 105-124.

Kröner, A., Hoffmann, J.E., Wong, J.M., Geng, H.-Y., Schneider, K.P., Xie, H., Yang, J.-H. and Nhleko, N., 2019. Archaean Crystalline Rocks of the Eastern Kaapvaal Craton. 1-32.

Laurent, O. and Zeh, A., 2015. A linear Hf isotope-age array despite different granitoid sources and complex Archean geodynamics: Example from the Pietersburg block (South Africa). Earth and Planetary Science Letters, 430, 326-338.

Laurent, O., Zeh, A., Brandl, G., Vezinet, A. and Wilson, A., 2019. Granitoids and Greenstone Belts of the Pietersburg Block—Witnesses of an Archaean Accretionary Orogen Along the Northern Edge of the Kaapvaal Craton, in: Kröner, A. and Hofmann, A. (Eds.), The Archaean geology of the Kaapvaal Craton, southern Africa. Springer, 83-107.

McCarthy, T.S., Corner, B., Lombard, H., Beukes, N.J., Armstrong, R.A. and Cawthorn, R.G., 2018. The pre-Karoo geology of the southern portion of the Kaapvaal Craton, South Africa. South African Journal of Geology, 121, 1-22.

Pidgeon, R.T., Nemchin, A.A., Roberts, M.P., Whitehouse, M.J. and Bellucci, J.J., 2019. The accumulation of non-formula elements in zircons during weathering: Ancient zircons from the Jack Hills, Western Australia. Chemical Geology, 530, 119310.

Poujol, M. and Anhaeusser, C.R., 2001. The Johannesburg Dome, South Africa: new single zircon U–Pb isotopic evidence for early Archaean granite–greenstone development within the central Kaapvaal Craton. Precambrian Research, 108, 139-157.

Poujol, M., Anhaeusser, C.R. and Armstrong, R.A., 2002. Episodic granitoid emplacement in the Archaean Amalia–Kraaipan terrane, South Africa: confirmation from single zircon U–Pb geochronology. Journal of African Earth Sciences, 35, 147-161.

Poujol, M., Hirner, A.J., Armstrong, R.A. and Anhaeusser, C.R., 2008. U-Pb SHRIMP data for the Madibe greenstone belt: implications for crustal growth on the western margin of the Kaapvaal Craton, South Africa. South African Journal of Geology, 111, 67-78.

Poujol, M., Kiefer, R., Robb, L.J., Anhaeusser, C.R. and Armstrong, R.A., 2005. New U-Pb data on zircons from the Amalia greenstone belt Southern Africa: insights into the Neoarchaean evolution of the Kaapvaal Craton. South African Journal of Geology, 108, 317-332.

Reimink, J.R., Davies, J.H.F.L., Bauer, A.M. and Chacko, T., 2020. A comparison between zircons from the Acasta Gneiss Complex and the Jack Hills region. Earth and Planetary Science Letters, 531, 115975.

Robb, L.J., Brandl, G., Anhaeusser, C.R. and Poujol, M., 2006. Archaean Granitoid Intrusions, in: Johnson, M.R., Anhaeusser, C.R.and Thomas, R.J. (Eds.), The

Geology of South Africa. Geological Society of South Africa, Johannesburg/Council for Geosciences, Pretoria,

Scherer, E.E., Munker, C. and Mezger, K., 2007. The Lu-Hf systematics of meteorites: Consistent or not? Geochimica et Cosmochimica Acta, 71, A888-A888.

Schwarz-Schampera, U., Terblanche, H. and Oberthür, T., 2010. Volcanic-hosted massive sulfide deposits in the Murchison greenstone belt, South Africa. Mineralium Deposita, 45, 113-145.

Zeh, A., Gerdes, A. and Barton, J.M., 2009. Archean Accretion and Crustal Evolution of the Kalahari Craton-the Zircon Age and Hf Isotope Record of Granitic Rocks from Barberton/Swaziland to the Francistown Arc. Journal of Petrology, 50, 933-966.

Zeh, A., Gerdes, A. and Millonig, L., 2011. Hafnium isotope record of the Ancient Gneiss Complex, Swaziland, southern Africa: evidence for Archaean crust-mantle formation and crust reworking between 3.66 and 2.73 Ga. Journal of the Geological Society, London, 168, 953-963.

Zeh, A., Jaguin, J., Poujol, M., Boulvais, P., Block, S. and Paquette, J.-L., 2013. Juvenile crust formation in the northeastern Kaapvaal Craton at 2.97 Ga—Implications for Archean terrane accretion, and the source of the Pietersburg gold. Precambrian Research, 233, 20-43.

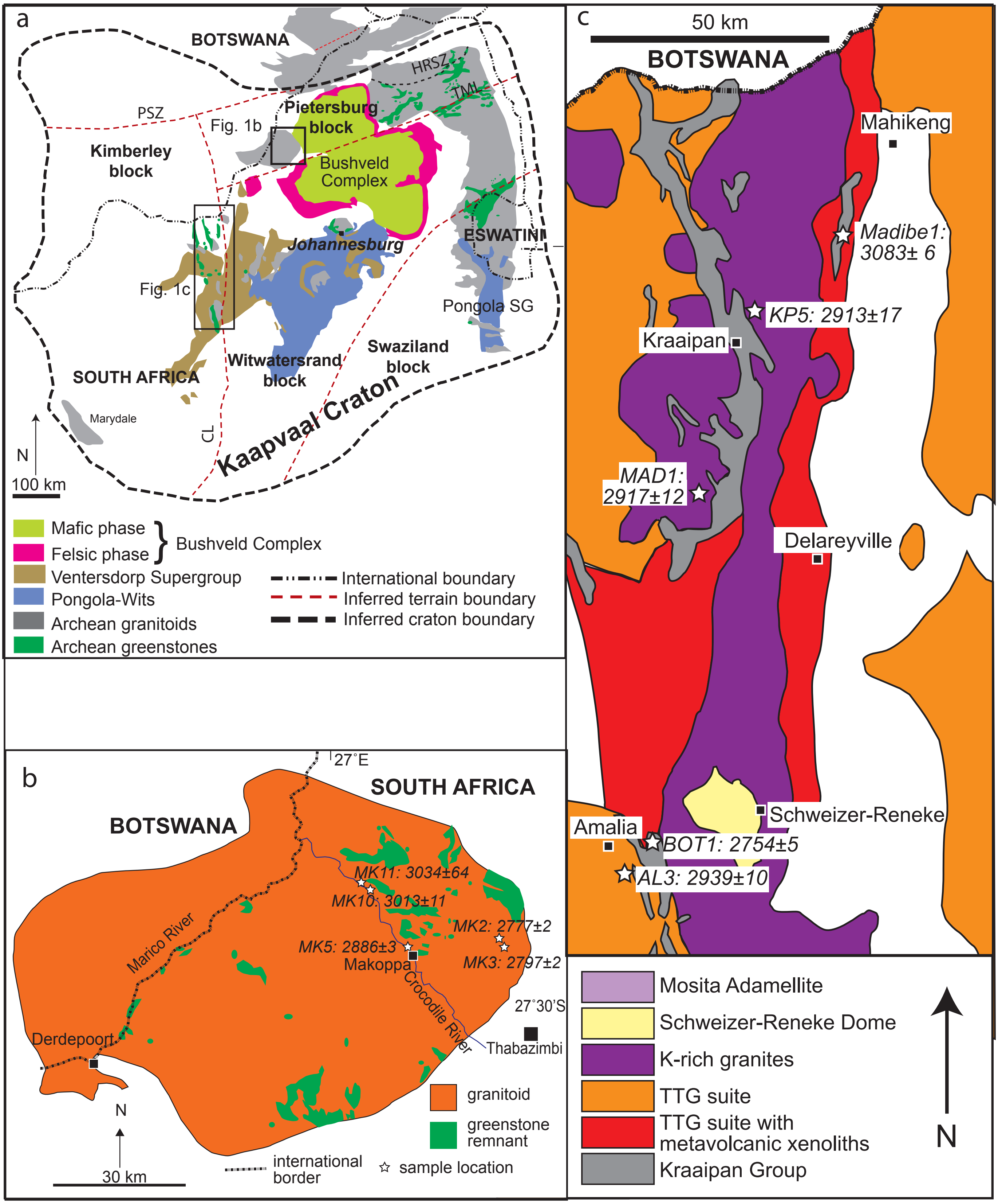

Figure 1 Elburg & Poujol

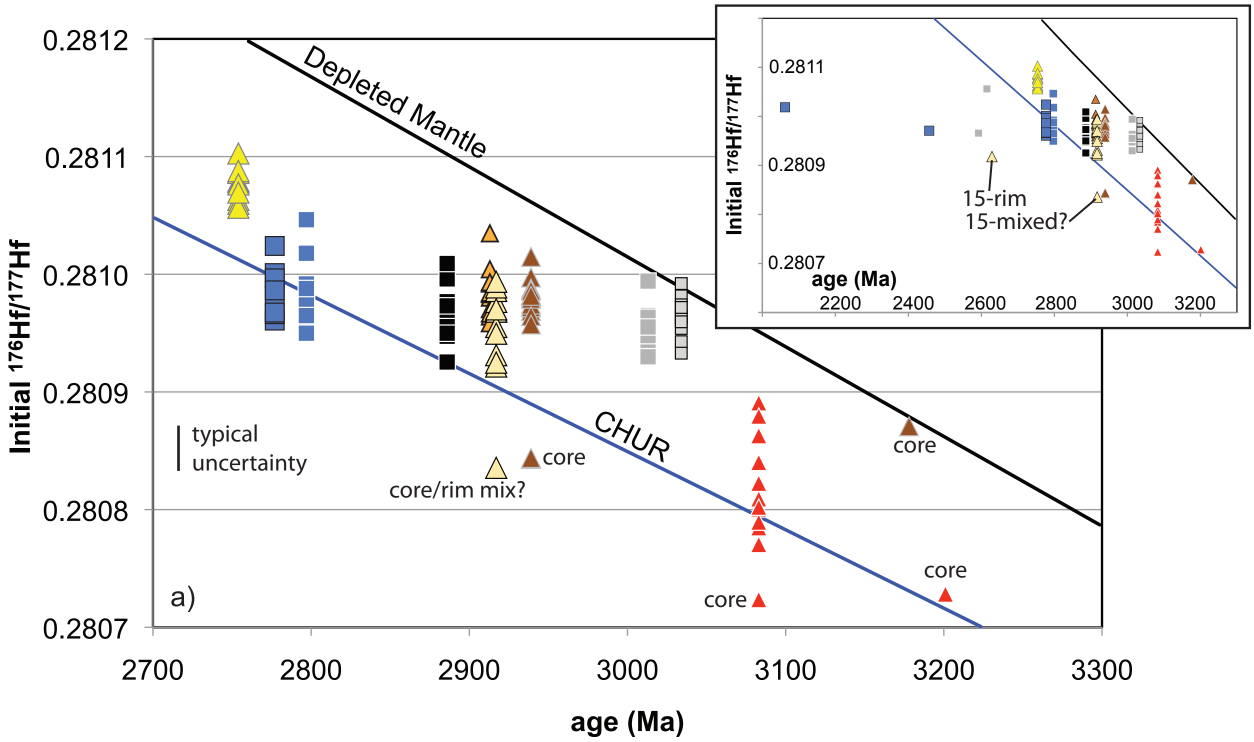

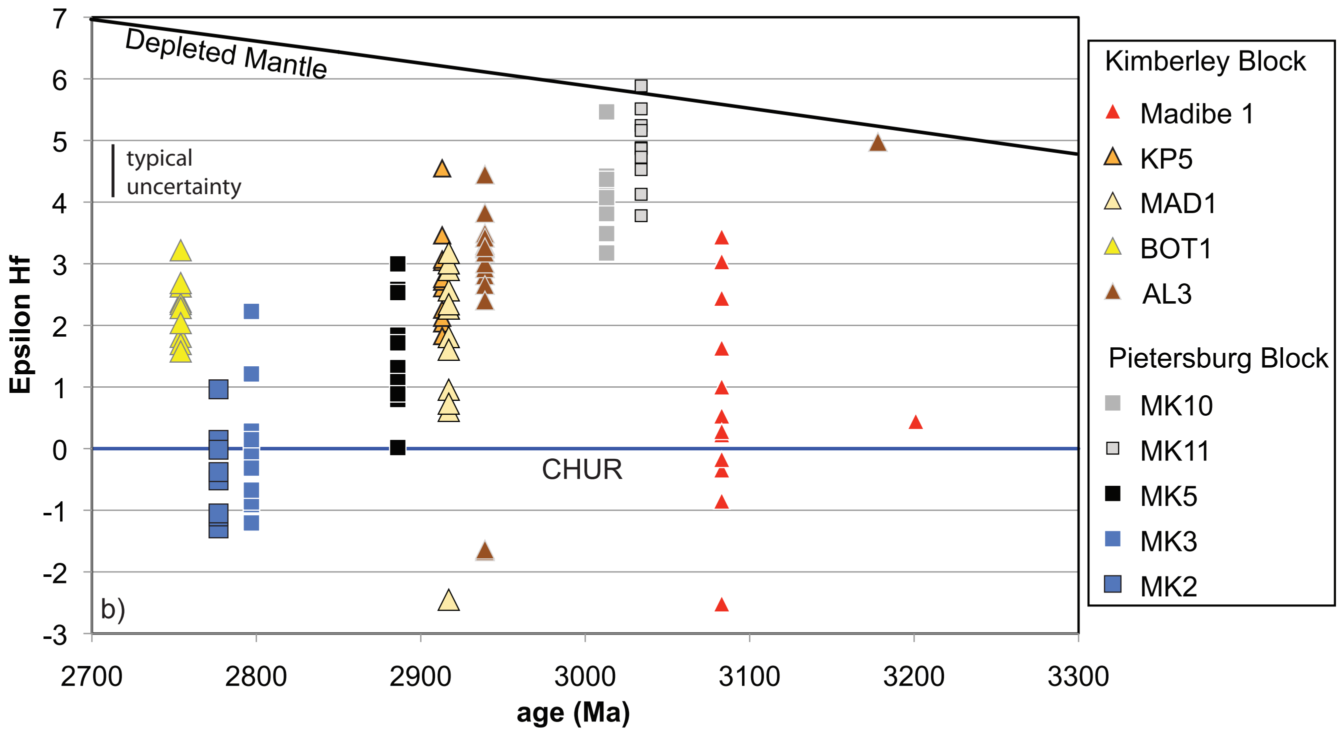

Figure 2 Elburg & Poujol

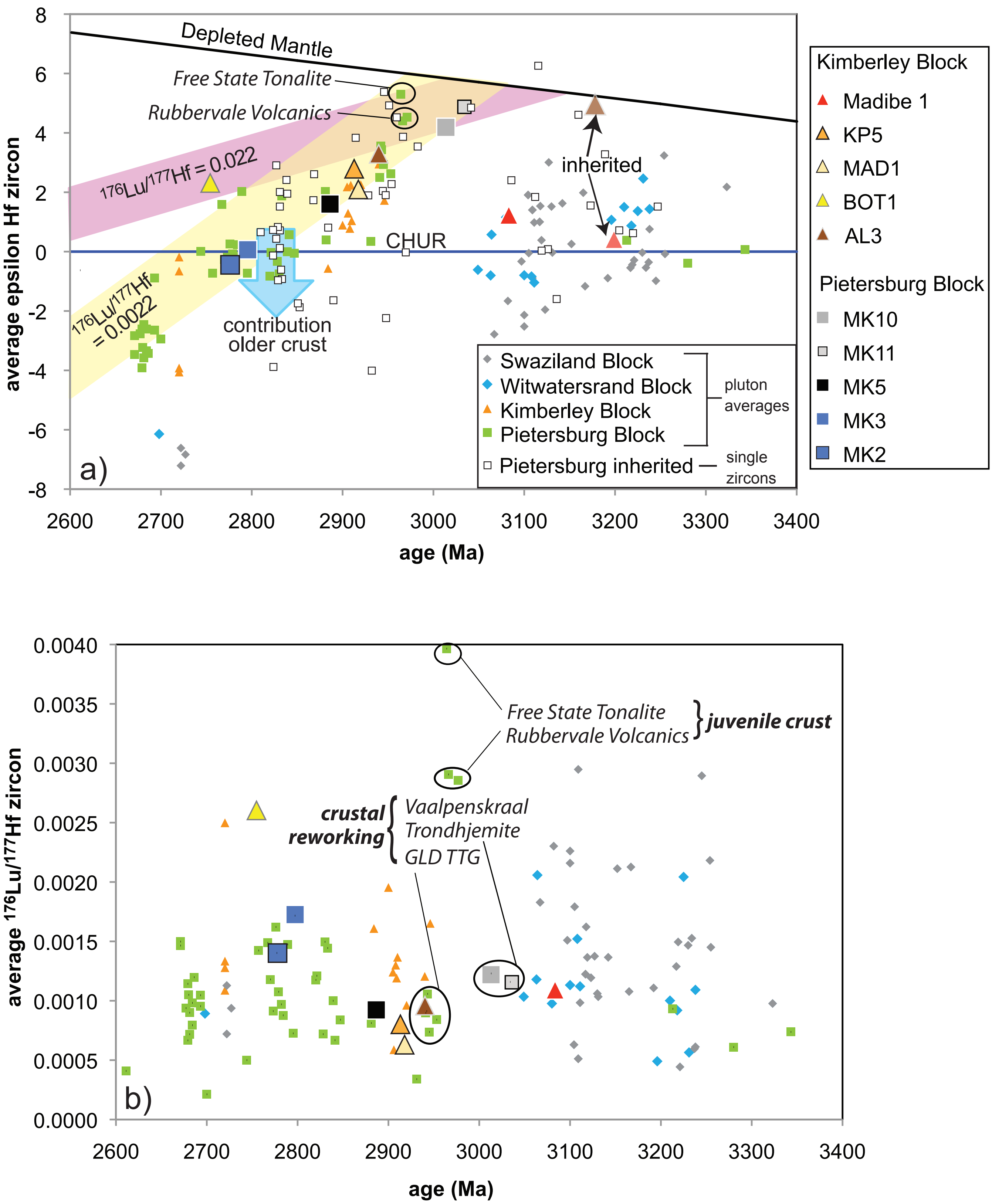

Figure 3 Elburg & Poujol

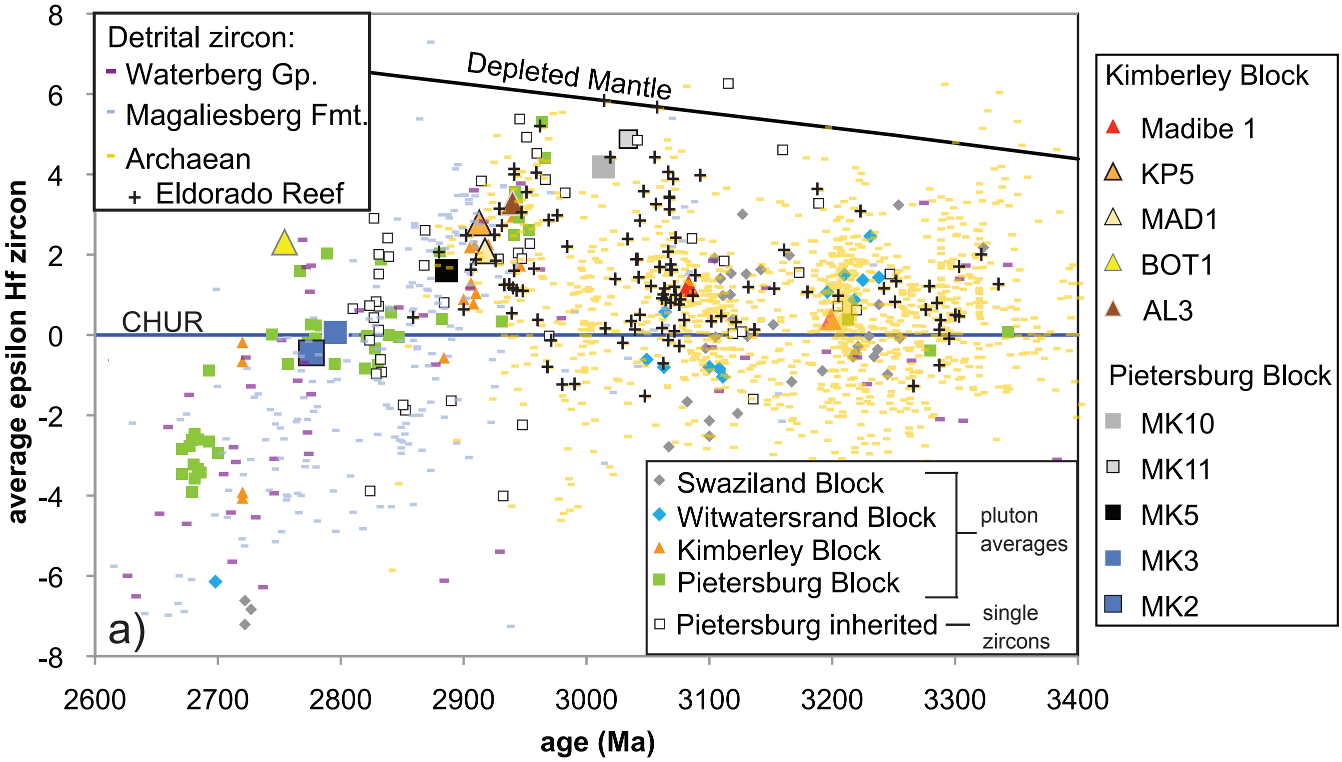

Detrital zircon:
Waterberg Gp.
Magaliesberg Fmt.
Archaean
+ Eldorado Reef
Depleted Mantle
CHUR
average epsilon Hf zircon
age (Ma)
a)
Swaziland Block
Witwatersrand Block
Kimberley Block
Pietersburg Block
pluton averages
Pietersburg inherited
single zircons
Kimberley Block
Madibe 1
KP5
MAD1
BOT1
AL3
Pietersburg Block
MK10
MK11
MK5
MK3
MK2

Table 1: Overview of analysed samples.

Sample name	**Area**	**Reference**	**Rock type**	**Age ± 2 SD (Ma)**	**Type of age**	**Dating technique**	**mean $^{176}Hf/^{177}Hf_i$**	**mean εHf$_i$ (± 2 SD)**	**T_{DM} mafic**	**T_{DM} tonalitic**
Pietersburg Block										
MK10	Makoppa Dome	Anhaeusser and Poujol (2004)	Vaalpenskraal trondhjemitic gneiss	3013 ± 11	wtd. av. 7/6	LA-ICP-MS	0.28096	4.2 ± 1.2	3.15	3.08
MK11	Makoppa Dome	Anhaeusser and Poujol (2004)	Vaalpenskraal trondhjemitic gneiss	3034 ± 64	wtd. av. 7/6	LA-ICP-MS	0.28096	4.9 ± 1.3	3.10	3.07
MK2	Makoppa Dome	Anhaeusser and Poujol (2004)	Rooibokvlei granodiorite/ monzogranite	2777 ± 2	upper intercept	ID-TIMS	0.28099	-0.4 ± 1.5	3.34	3.05
MK3	Makoppa Dome	Anhaeusser and Poujol (2004)	Rooibokvlei granodiorite/ monzogranite	2797 ± 2	upper intercept	ID-TIMS	0.28099	0.1 ± 2	3.31	3.05
MK5	Makoppa Dome	Anhaeusser and Poujol (2004)	Makoppa granodiorite/ monzogranite	2886 +3/-2	upper intercept	ID-TIMS	0.28097	1.6 ± 1.9	3.26	3.07
Kimberley Block										
MADIBE1	Kraaipan	Poujol et al. (2008)	quartz-sericite schist	3083 ± 6	wtd. av. 7/6	SHRIMP	0.28083	1.2 ± 3.0	3.43	3.25
			core	3201 ± 4	$^{207}Pb/^{206}Pb$	SHRIMP	0.28073	0.4 ± 0.9	3.72	3.40
BOT1	Amalia	Poujol et al. (2005)	accretionary lapilli tuff	2754 ± 5	wtd. av. 7/6	SHRIMP	0.28108	2.3 ± 1.0	3.11	2.93
MAD1	Kraaipan	Poujol et al. (2002)	grey granodiorite	2917 ± 9	wtd. av. 7/6	SHRIMP	0.28096	2.0 ±1.8	3.25	3.08
KP5	Kraaipan	Poujol et al. (2002)	pink granodiorite	2913 ± 17	wtd. av. 7/6	SHRIMP	0.28098	2.8 ± 1.5	3.19	3.05
AL3	Amalia	Poujol et al. (2002)	leuco-trondhjemite gneiss	2939 ± 10	wtd. av. 7/6	SHRIMP	0.28098	3.2 ± 1.0	3.22	3.08
			core	3178 ± 10	$^{207}Pb/^{206}Pb$	SHRIMP	0.28087	5.0 ± 1.0	3.20	3.19

wtd. av. 7/6 = weighted average $^{207}Pb/^{206}Pb$ age

T_{DM} = depleted mantle extraction age in Ga; calculated with $^{176}Lu/^{177}Hf$ = 0.022 for mafic protoliths, and 0.0022 for felsic protoliths

Sample	$^{176}Hf/^{177}Hf$	SE	$^{178}Hf/^{177}Hf$	SE	$^{178}Hf/^{177}Hf$	SE	$^{180}Hf/^{177}Hf$	SE	$^{176}Lu/^{177}Hf$	SE	$^{176}Yb/^{177}Hf$	SE	AGE (years)	Initial $^{176}Hf/^{177}Hf$	INITIAL EPSILON	average	2SD	average epsilon Hf	2SD epsilon Hf	median	median epsilon Hf	TDM2a (Ga)	TDM2b (Ga)		TDM2a	TDM2b
																								$^{176}Hf/^{177}Hf_{DM}$	0.28325	0.28325
																								$^{176}Lu/^{177}Hf_{DM}$	0.0388	0.0388
																								$^{176}Lu/^{177}Hf_{crust}$	0.022	0.0022
MADIBE1-01	0.280859	0.000008	0.008659	0.000008	1.467286	0.000012	1.886852	0.000030	0.0010	0.00000	0.032922	0.000078	3.083E+09	0.280802	0.3	0.280828	8.34057E-05	1.2	3.0	0.280809	0.5	3.43	3.25		3.499	3.288
MADIBE1-08	0.280924	0.000009	0.008666	0.000008	1.467275	0.000013	1.886802	0.000028	0.0008	0.00000	0.022453	0.000133	3.083E+09	0.280879	3.0										3.284	3.182
MADIBE1-11	0.280920	0.000007	0.008683	0.000008	1.467302	0.000010	1.886807	0.000024	0.0016	0.00001	0.054102	0.000236	3.083E+09	0.280822	1.0										3.443	3.260
MADIBE1-A	0.280933	0.000010	0.008715	0.000011	1.467265	0.000014	1.886846	0.000034	0.0007	0.00001	0.023107	0.000307	3.083E+09	0.280891	3.4										3.252	3.166
MADIBE1-B	0.280913	0.000016	0.008673	0.000017	1.467367	0.000019	1.886821	0.000036	0.0008	0.00001	0.025872	0.000392	3.083E+09	0.280863	2.4										3.330	3.204
MADIBE1-C	0.280872	0.000009	0.008656	0.000008	1.467283	0.000012	1.886874	0.000026	0.0011	0.00000	0.036333	0.000099	3.083E+09	0.280809	0.5										3.480	3.278
MADIBE1-D	0.280840	0.000008	0.008666	0.000008	1.467246	0.000012	1.886809	0.000024	0.0012	0.00001	0.038676	0.000205	3.083E+09	0.280770	-0.8										3.588	3.331
MADIBE1-E	0.280848	0.000008	0.008669	0.000008	1.467252	0.000010	1.886811	0.000022	0.0010	0.00000	0.031665	0.000090	3.083E+09	0.280789	-0.2										3.535	3.305
MADIBE1-F	0.280848	0.000007	0.008674	0.000007	1.467286	0.000010	1.886834	0.000023	0.0011	0.00001	0.034186	0.000187	3.083E+09	0.280785	-0.3										3.548	3.312
MADIBE1-G	0.280927	0.000010	0.008668	0.000009	1.467290	0.000012	1.886772	0.000034	0.0008	0.00000	0.028802	0.000123	3.083E+09	0.280880	3.0										3.283	3.181
MADIBE1-I	0.280885	0.000010	0.008649	0.000009	1.467274	0.000013	1.886826	0.000027	0.0014	0.00002	0.050544	0.000525	3.083E+09	0.280801	0.2										3.504	3.290
MADIBE1-L	0.280913	0.000009	0.008646	0.000009	1.467303	0.000015	1.886817	0.000032	0.0012	0.00001	0.041667	0.000531	3.083E+09	0.280840	1.6										3.394	3.236
MADIBE1-K-core	*0.280802*	*0.000010*	*0.008655*	*0.000012*	*1.467271*	*0.000016*	*1.886847*	*0.000033*	*0.0013*	*0.00005*	*0.047083*	*0.001760*	*3.083E+09*	*0.280724*	*-2.5*										3.718	3.395
MADIBE1-J	*0.280797*	*0.000010*	*0.008660*	*0.000010*	*1.467277*	*0.000017*	*1.886817*	*0.000033*	*0.0011*	*0.00001*	*0.039394*	*0.000188*	*3.201E+09*	*0.280728*	*0.4*										3.569	3.382
BOT1-01	0.281222	0.000009	0.008670	0.000012	1.467301	0.000012	1.886867	0.000025	0.0029	0.00001	0.109723	0.000570	2.754E+09	0.281069	2.0	0.281076	2.83753E-05	2.3	1.0	0.281077	2.3	3.11	2.93		3.132	2.939
BOT1-A	0.281240	0.000009	0.008650	0.000010	1.467276	0.000011	1.886811	0.000025	0.0031	0.00001	0.119893	0.000196	2.754E+09	0.281076	2.3										3.112	2.929
BOT1-B	0.281209	0.000010	0.008665	0.000012	1.467274	0.000012	1.886847	0.000027	0.0023	0.00000	0.088091	0.000155	2.754E+09	0.281088	2.7										3.080	2.913
BOT1-C	0.281222	0.000013	0.008719	0.000015	1.467292	0.000018	1.886832	0.000043	0.0023	0.00001	0.080906	0.000812	2.754E+09	0.281103	3.2										3.038	2.893
BOT1-D	0.281199	0.000013	0.008685	0.000014	1.467322	0.000014	1.886851	0.000031	0.0027	0.00002	0.096995	0.000346	2.754E+09	0.281056	1.6										3.168	2.956
BOT1-E	0.281218	0.000010	0.008646	0.000010	1.467308	0.000012	1.886810	0.000026	0.0026	0.00001	0.102671	0.000318	2.754E+09	0.281078	2.3										3.107	2.927
BOT1-F	0.281246	0.000011	0.008632	0.000013	1.467292	0.000013	1.886801	0.000029	0.0035	0.00000	0.144254	0.000329	2.754E+09	0.281060	1.7										3.159	2.952
BOT1-H	0.281178	0.000012	0.008717	0.000012	1.467346	0.000016	1.886918	0.000037	0.0017	0.00001	0.065582	0.000122	2.754E+09	0.281086	2.6										3.085	2.916
BOT1-I	0.281200	0.000010	0.008680	0.000012	1.467325	0.000012	1.886863	0.000026	0.0026	0.00001	0.100607	0.000715	2.754E+09	0.281063	1.8										3.149	2.947
BOT1-L	0.281181	0.000017	0.008685	0.000016	1.467289	0.000023	1.886877	0.000049	0.0019	0.00005	0.075724	0.001310	2.754E+09	0.281079	2.4										3.104	2.925
BOT1-J	*0.281941*	*0.000010*	*0.008665*	*0.000011*	*1.467273*	*0.000015*	*1.886800*	*0.000034*	*0.0014*	*0.00004*	*0.056612*	*0.001480*	*2.754E+09*	*0.281865*	*30.3*											
BOT1-K	*0.282416*	*0.000010*	*0.008705*	*0.000010*	*1.467299*	*0.000015*	*1.886930*	*0.000033*	*0.0005*	*0.00001*	*0.017131*	*0.000188*	*2.754E+09*	*0.282392*	*49.1*											
BOT1-M	*0.281750*	*0.000008*	*0.008653328*	*0.00000758*	*1.46728*	*0.0000116*	*1.886845*	*0.0000274*	*0.0009*	*0.00001*	*0.03511366*	*0.000211*	*2.754E+09*	*0.281701*	*24.5*											
MAD1-A	0.281013	0.000013	0.008660115	0.0000117	1.467303	0.0000156	1.886823	0.000033	0.0003	0.00000	0.01465444	0.00028	2.917E+09	0.280994	3.2	0.280961	4.9698E-05	2.0	1.8	0.280968	2.3	3.25	3.08		3.156	3.034
MAD1-B	0.280992	0.000014	0.008644897	0.0000129	1.467307	0.0000178	1.886903	0.0000414	0.0008	0.00001	0.03208008	0.000486	2.917E+09	0.280949	1.6										3.280	3.095
MAD1-C	0.280988	0.000009	0.008671111	0.00000831	1.467317	0.0000131	1.886959	0.0000283	0.0003	0.00000	0.01197282	0.000102	2.917E+09	0.280970	2.3										3.221	3.066
MAD1-D	0.280959	0.000011	0.0086237	0.0000106	1.467273	0.0000137	1.886948	0.0000332	0.0006	0.00000	0.02392832	0.000161	2.917E+09	0.280925	0.7										3.348	3.129
MAD1-E	0.280987	0.000009	0.008665994	0.00000937	1.467286	0.0000115	1.886794	0.0000246	0.0012	0.00001	0.0520325	0.000426	2.917E+09	0.280922	0.6										3.358	3.133
MAD1-F	0.281022	0.000011	0.008637976	0.0000104	1.467257	0.0000153	1.886865	0.0000324	0.0006	0.00000	0.02413174	0.000152	2.917E+09	0.280989	3.0										3.169	3.040
MAD1-G	0.281017	0.000013	0.008671968	0.0000123	1.467274	0.0000175	1.886883	0.000037	0.0006	0.00000	0.02296585	0.000144	2.917E+09	0.280986	2.9										3.178	3.045
MAD1-H	0.280981	0.000010	0.008665103	0.0000109	1.467299	0.0000141	1.886885	0.0000322	0.0005	0.00000	0.01720286	0.0000972	2.917E+09	0.280955	1.8										3.263	3.087
MAD1-I	0.280965	0.000010	0.008649166	0.0000107	1.467308	0.000013	1.886772	0.0000309	0.0006	0.00000	0.02363968	0.000122	2.917E+09	0.280931	1.0										3.331	3.120
MAD1-J	0.281035	0.000015	0.008625743	0.000015	1.467235	0.0000181	1.886839	0.0000388	0.0012	0.00002	0.05037008	0.000961	2.917E+09	0.280968	2.3										3.227	3.069
MAD1-K	0.280991	0.000009	0.008657792	0.00000766	1.467263	0.0000121	1.886884	0.0000276	0.0004	0.00000	0.01573216	0.000163	2.917E+09	0.280968	2.3										3.227	3.069
MAD1-L	0.280995	0.000009	0.008693356	0.00000941	1.467259	0.0000128	1.886815	0.0000308	0.0003	0.00000	0.01204865	0.0000746	2.917E+09	0.280977	2.6										3.204	3.057
MAD1-15-CORE	*0.280878*	*0.000010*	*0.008688953*	*0.0000099*	*1.467307*	*0.0000122*	*1.886812*	*0.0000281*	*0.0008*	*0.00001*	*0.0251479*	*0.000298*	*2.917E+09*	*0.280836*	*-2.5*										3.598	3.251
MAD1-15-RIM	*0.280957*	*0.000010*	*0.008651547*	*0.00000891*	*1.46727*	*0.000012*	*1.88678*	*0.0000278*	*0.0008*	*0.00000*	*0.03149061*	*0.000183*	*2.629E+09*	*0.280918*	*-6.3*										*3.704*	*3.154*
KP5-01	0.281033	0.000011	0.008659432	0.0000102	1.46728	0.0000143	1.886775	0.0000314	0.0007	0.00001	0.02698622	0.000252	2.913E+09	0.280993	3.1	0.280985	4.33037E-05	2.8	1.5	0.280983	2.7	3.19	3.05		3.161	3.035
KP5-A	0.280993	0.000012	0.00862756	0.0000124	1.467244	0.0000152	1.886796	0.0000343	0.0005	0.00000	0.02052981	0.000064	2.913E+09	0.280967	2.1										3.236	3.071
KP5-B	0.281057	0.000016	0.008591597	0.000019	1.467236	0.0000202	1.886731	0.000043	0.0013	0.00003	0.07250861	0.00216	2.913E+09	0.280984	2.8										3.186	3.047
KP5-C	0.281013	0.000013	0.008640955	0.0000135	1.467279	0.0000173	1.886842	0.0000375	0.0008	0.00001	0.0327433	0.000467	2.913E+09	0.280970	2.3										3.226	3.066
KP5-D	0.280976	0.000010	0.008654982	0.00000889	1.467275	0.0000129	1.886881	0.0000309	0.0003	0.00000	0.01326036	0.0000655	2.913E+09	0.280958	1.8										3.259	3.083
KP5-E	0.280995	0.000010	0.008628596	0.0000103	1.467261	0.0000128	1.88682	0.0000298	0.0005	0.00000	0.02235655	0.000215	2.913E+09	0.280964	2.0										3.243	3.075
KP5-F	0.281047	0.000011	0.008634253	0.0000102	1.467257	0.0000139	1.886743	0.0000312	0.0008	0.00001	0.03600648	0.000232	2.913E+09	0.281004	3.5										3.130	3.020
KP5-G	0.281064	0.000013	0.008520501	0.0000131	1.467199	0.0000145	1.8867	0.000034	0.0014	0.00001	0.06959379	0.00067	2.913E+09	0.280983	2.7										3.190	3.049
KP5-H	0.281010	0.000010	0.008661451	0.00000995	1.467319	0.0000147	1.88693	0.0000306	0.0005	0.00000	0.02264225	0.000218	2.913E+09	0.280980	2.6										3.198	3.053
KP5-I	0.281106	0.000011	0.008496207	0.0000122	1.467214	0.0000139	1.886618	0.000028	0.0013	0.00001	0.06039746	0.000474	2.913E+09	0.281035	4.5										3.044	2.977
KP5-J	0.281015	0.000012	0.008653422	0.0000133	1.467322	0.0000162	1.886862	0.0000337	0.0004	0.00001	0.01902001	0.000357	2.913E+09	0.280992	3.0										3.165	3.036
AL3-13CORE	0.281032	0.000012	0.00865982	0.000011	1.467296	0.0000148	1.886855	0.0000328	0.0009	0.00002	0.03095853	0.000599	2.939E+09	0.280981616	3.3	0.280981	2.93619E-05	3.2	1.0	0.280979	3.2	3.22	3.08		3.164	3.049
AL3-01CORE	0.281007	0.000011	0.008656562	0.0000112	1.467276	0.0000137	1.886827	0.0000342	0.0009	0.00000	0.03105362	0.000142	2.939E+09	0.280957313	2.4										3.232	3.083
AL3-15CORE	0.281032	0.000012	0.008628639	0.0000123	1.467248	0.0000137	1.886787	0.0000325	0.0012	0.00002	0.04098378	0.000639	2.939E+09	0.280964415	2.7										3.212	3.073
AL3-A	0.281030	0.000008	0.008682347	0.00000777	1.467282	0.0000106	1.886879	0.0000249	0.0009	0.00002	0.03045036	0.000779	2.939E+09	0.280979174	3.2										3.171	3.053
AL3-B	0.281041	0.000007	0.008670842	0.00000712	1.467268	0.0000101	1.886844	0.000023	0.0010	0.00001	0.03179263	0.000365	2.939E+09	0.280985968	3.4										3.152	3.043
AL3-D	0.281037	0.000006	0.008658987	0.00000588	1.467257	0.00000988	1.886809	0.0000204	0.0010	0.00001	0.03363031	0.000355	2.939E+09	0.280982549	3.3										3.161	3.048
AL3-E	0.281048	0.000005	0.008664814	0.00000522	1.467273	0.00000854	1.886843	0.0000193	0.0013	0.00003	0.04631771	0.000962	2.939E+09	0.280974203	3.0										3.185	3.059
AL3-F	0.281027	0.000007	0.008676255	0.00000655	1.467293	0.0000107	1.886825	0.000024	0.0008	0.00000	0.02873864	0.0000726	2.939E+09	0.280981044	3.2										3.165	3.050
AL3-G	0.281059	0.000013	0.008713671	0.000014	1.467328	0.0000176	1.886766	0.0000365	0.0008	0.00000	0.02928768	0.000122	2.939E+09	0.281014701	4.4										3.071	3.004
AL3-H	0.281046	0.000007	0.00867414	0.00000692	1.467284	0.0000104	1.886856	0.0000235	0.0010	0.00000	0.03631203	0.0000443	2.939E+09	0.280987881	3.5										3.146	3.041
AL3-I	0.281040	0.000009	0.008696171	0.00000925	1.467277	0.0000136	1.88688	0.0000313	0.0008	0.00003	0.02754151	0.00118	2.939E+09	0.280997231	3.8										3.120	3.028
AL3-J	0.281028	0.000009	0.008655202	0.00000838	1.467277	0.0000141	1.886762	0.0000291	0.0010	0.00001	0.0361459	0.00024	2.939E+09	0.280972008	2.9										3.191	3.062
AL3-L	0.281018	0.000009	0.008657296	0.00000735	1.467272	0.0000119	1.886826	0.0000296	0.0009	0.00001	0.02939025	0.0003	2.939E+09	0.280968808	2.8										3.200	3.067
AL3-C-core	*0.281027*	*0.000007*	*0.008650516*	*0.00000822*	*1.467285*	*0.00000972*	*1.886896*	*0.0000229*	*0.0032*	*0.00002*	*0.119943*	*0.000543*	*2.939E+09*	*0.280843823*	*-1.6*										3.550	3.239
AL3-K-core	*0.280958*	*0.000007*	*0.008673709*	*0.00000789*	*1.467307*	*0.00000976*	*1.886932*	*0.0000211*	*0.0020*	*0.00001*	*0.05622789*	*0.000377*	*2.939E+09*	*0.280843053*	*-1.7*										3.552	3.240
AL3-12	*0.280976*	*0.000011*	*0.008712668*	*0.0000105*	*1.467294*	*0.0000116*	*1.886898*	*0.0000285*	*0.0017*	*0.00001*	*0.0635719*	*0.000577*	*3.178E+09*	*0.280870757*	*5.0*										3.199	3.188
MK11-02CORE	0.281021	0.000010	0.00865807	0.0000107	1.467252	0.0000128	1.886808	0.0000323	0.0008	0.00000	0.03311846	0.000106	3.034E+09	0.280971777	5.2	0.280964	3.52639E-05	4.9	1.3	0.280964	4.9	3.10	3.07		3.082	3.057
MK11-A	0.281019	0.000014	0.008599006	0.0000147	1.467285	0.0000151	1.886857	0.0000343	0.0015	0.00001	0.05280675	0.000196	3.034E+09	0.280932937	3.8										3.191	3.111
MK11-B	0.281053	0.000011	0.00871028	0.0000108	1.467285	0.0000129	1.886799	0.0000316	0.0010	0.00001	0.04195169	0.000409	3.034E+09	0.280992076	5.9										3.025	3.029
MK11-C	0.281016	0.000010	0.008667863	0.0000113	1.467262	0.0000138	1.886756	0.0000317	0.0007	0.00001	0.02588409	0.000366	3.034E+09	0.280974024	5.2										3.075	3.054
MK11-D	0.281015	0.000010	0.008637293	0.00000983	1.467288	0.0000137	1.886901	0.0000269	0.0009	0.00001	0.03306196	0.000412	3.034E+09	0.280959598	4.7										3.116	3.074
MK11-E	0.281041	0.000013	0.008641857	0.0000132	1.467285	0.0000157	1.886914	0.0000367	0.0017	0.00000	0.05637877	0.000165	3.034E+09	0.280942692	4.1										3.163	3.097
MK11-F	0.281022	0.000013	0.008665755	0.0000138	1.467271	0.0000146	1.886941	0.000036	0.0012	0.00000	0.03959787	0.0000923	3.034E+09	0.280953943	4.5										3.132	3.082
MK11-G	0.281027	0.000010	0.00866709	0.0000113	1.467276	0.0000144	1.886845	0.00003	0.0011	0.00000	0.04208675	0.000113	3.034E+09	0.280963485	4.9										3.105	3.069
MK11-H	0.281045	0.000009	0.008665337	0.00000975	1.467279	0.0000124	1.886888	0.0000276	0.0011	0.00000	0.03793004	0.00011	3.034E+09	0.280981623	5.5										3.054	3.044
MK11-I	0.281053	0.000013	0.008675965	0.0000151	1.46725	0.0000158	1.886764	0.0000339	0.0015	0.00001	0.05600073	0.000255	3.034E+09	0.280963908	4.9										3.104	3.068
MK5-A	0.280993	0.000012	0.008653005	0.0000101	1.46729	0.0000136	1.886771	0.000032	0.0008	0.00001	0.02834525	0.000369	2.886E+09	0.28094989	0.9	0.280969	5.24925E-05	1.6	1.9	0.280967	1.5	3.26	3.07		3.314	3.096
MK5-B	0.281037	0.000009	0.00868478	0.00000818	1.467241	0.0000121	1.886858	0.000027	0.0005	0.00000	0.01713856	0.00003	2.886E+09	0.281009132	3.0										3.148	3.014
MK5-C	0.281007	0.000008	0.008669968	0.00000827	1.467268	0.0000134	1.886875	0.0000285	0.0006	0.00000	0.02193006	0.000182	2.886E+09	0.280973139	1.7										3.249	3.064
MK5-D	0.281060	0.000010	0.008714261	0.0000108	1.467303	0.0000134	1.886865	0.0000315	0.0012	0.00001	0.04238175	0.000425	2.886E+09	0.280996049	2.5										3.185	3.032
MK5-E	0.281015	0.000009	0.008677207	0.00000948	1.467235	0.0000121	1.886798	0.0000286	0.0007	0.00000	0.02514613	0.000176	2.886E+09	0.280976664	1.8										3.239	3.059
MK5-F	0.280999	0.000010	0.008643025	0.00000957	1.467269	0.0000122	1.886876	0.0000277	0.0008	0.00000	0.03034146	0.000132	2.886E+09	0.280955479	1.1										3.299	3.088
MK5-G	0.281039	0.000010	0.008681263	0.0000101	1.467276	0.0000143	1.886832	0.000032	0.0008	0.00000	0.02829921	0.000213	2.886E+09	0.280997515	2.6										3.181	3.030
MK5-H	0.280994	0.000011	0.008647666	0.0000106	1.46725	0.0000145	1.886825	0.0000295	0.0008	0.00000	0.03177566	0.000136	2.886E+09	0.280947312	0.8										3.322	3.099
MK5-I	0.281083	0.000010	0.008673173	0.0000118	1.467298	0.0000124	1.886838	0.0000295	0.0022	0.00001	0.08419213	0.000281	2.886E+09	0.280961851	1.3										3.281	3.079
MK5-J	0.280972	0.000011	0.00859856	0.0000112	1.467246	0.0000137	1.886839	0.0000317	0.0008	0.00000	0.03130875	0.0000679	2.886E+09	0.280925414	0.0										3.383	3.130
MK3-M	0.281106	0.000013	0.008650671	0.0000146	1.467282	0.0000133	1.886761	0.0000361	0.0026	0.00003	0.1093033	0.00117	2.797E+09	0.280964873	-0.7	0.280987	5.7418E-05	0.1	2.0	0.280985	0.0	3.31	3.05		3.376	3.080
MK3-A	0.281063	0.000011	0.008680162	0.0000114	1.467278	0.0000145	1.886789	0.000033	0.0014	0.00001	0.05252635	0.000501	2.797E+09	0.280987879	0.1										3.311	3.049
MK3-B	0.281045	0.000008	0.008689893	0.00000686	1.467274	0.0000121	1.886816	0.0000234	0.0010	0.00001	0.0319162	0.000338	2.797E+09	0.280991772	0.3										3.300	3.043
MK3-C	0.281011	0.000008	0.008627835	0.00000749	1.467243	0.0000108	1.886843	0.0000255	0.0011	0.00002	0.03929636	0.000634	2.797E+09	0.280949907	-1.2										3.418	3.101
MK3-D	0.281038	0.000009	0.008648747	0.00000821	1.467272	0.0000108	1.886875	0.0000245	0.0015	0.00002	0.05323365	0.000664	2.797E+09	0.280959475	-0.9										3.391	3.088
MK3-L	0.281102	0.000009	0.008662932	0.00000883	1.467295	0.0000112	1.886922	0.0000218	0.0024	0.00003	0.09101119	0.00107	2.797E+09	0.280974915	-0.3										3.348	3.067
MK3-E	0.281051	0.000009	0.008658271	0.00000827	1.467269	0.0000116	1.88678	0.0000257	0.0013	0.00001	0.05103226	0.00018	2.797E+09	0.28098155	-0.1										3.329	3.057
MK3-F	0.281089	0.000010	0.008693788	0.0000101	1.467262	0.0000122	1.886887	0.000025	0.0024	0.00001	0.08136618	0.000388	2.797E+09	0.280958268	-0.9										3.394	3.089
MK3-G	0.281087	0.000007	0.008666994	0.00000652	1.467277	0.00000996	1.886885	0.0000227	0.0013	0.00000	0.04334344	0.000145	2.797E+09	0.281017843	1.2										3.227	3.007
MK3-H	0.281169	0.000010	0.008674303	0.0000113	1.46727	0.0000126	1.886869	0.0000273	0.0023	0.00002	0.08349571	0.000635	2.797E+09	0.281046352	2.2										3.147	2.968
MK3-I	0.281133	0.000009	0.00864061	0.0000101	1.467215	0.0000119	1.886821	0.0000275	0.0022	0.00001	0.0820808	0.000326	2.797E+09	0.281017465	1.2										3.228	3.008
MK3-J	0.281052	0.000009	0.0086771	0.00000823	1.467292	0.0000105	1.886908	0.0000249	0.0011	0.00000	0.0425914	0.000191	2.797E+09	0.280991096	0.3										3.302	3.044
MK10-04-02	0.281018	0.000008	0.008671822	0.00000807	1.467265	0.0000116	1.886851	0.0000241	0.0011	0.00000	0.04382395	0.000202	3.013E+09	0.280955105	4.1	0.280958	3.46384E-05	4.2	1.2	0.280959	4.2	3.15	3.08		3.153	3.082
MK10-A	0.281031	0.000009	0.008646024	0.00000965	1.467301	0.0000115	1.886834	0.000027	0.0012	0.00000	0.04682708	0.000147	3.013E+09	0.280963437	4.4										3.129	3.070
MK10-B	0.281006	0.000008	0.008659644	0.00000905	1.467261	0.0000117	1.88685	0.0000249	0.0010	0.00001	0.04195067	0.000443	3.013E+09	0.280947841	3.8										3.173	3.092
MK10-C	0.281081	0.000010	0.008671172	0.0000111	1.46727	0.0000115	1.886867	0.0000278	0.0020	0.00002	0.08625252	0.000918	3.013E+09	0.280964919	4.4										3.125	3.068
MK10-E	0.281015	0.000013	0.008635629	0.0000123	1.467302	0.000015	1.886894	0.0000322	0.0015	0.00001	0.05525993	0.00044	3.013E+09	0.280929895	3.2										3.223	3.116
MK10-F	0.281021	0.000008	0.008658549	0.00000721	1.467267	0.0000116	1.886814	0.000026	0.0005	0.00000	0.01608989	0.0000988	3.013E+09	0.280994194	5.5										3.043	3.028
MK10-G	0.281014	0.000009	0.008690074	0.00000932	1.467283	0.0000128	1.886852	0.0000274	0.0010	0.00001	0.03672857	0.000284	3.013E+09	0.280958306	4.2										3.144	3.077
MK10-I	0.281019	0.000008	0.008651166	0.00000872	1.467295	0.0000112	1.886848	0.0000267	0.0010	0.00001	0.04199073	0.000411	3.013E+09	0.280959445	4.2										3.141	3.076
MK10-J	0.281098	0.000009	0.008658589	0.00000903	1.467263	0.0000111	1.8869	0.0000251	0.0023	0.00001	0.08754873	0.000306	3.013E+09	0.280964168	4.4										3.127	3.069
MK10-K	0.280985	0.000012	0.008679208	0.0000113	1.467342	0.0000175	1.886888	0.0000322	0.0008	0.00001	0.02856003	0.000259	3.013E+09	0.280938711	3.5										3.199	3.104
MK10-04-02-bis	*0.281113*	*0.000011*	*0.00868212*	*0.0000106*	*1.467263*	*0.0000146*	*1.886767*	*0.0000322*	*0.0011*	*0.00001*	*0.04001316*	*0.000261*	*2.615E+09*	*0.281056035*	*-1.7*										*3.332*	*2.965*
MK10-14	*0.281001*	*0.000010*	*0.008656418*	*0.00000922*	*1.467234*	*0.0000135*	*1.886828*	*0.0000291*	*0.0007*	*0.00000*	*0.02412591*	*0.0000446*	*2.592E+09*	*0.280965818*	*-5.4*										*3.613*	*3.091*
MK2-13.1	0.281050	0.000012	0.008648236	0.0000121	1.467285	0.0000135	1.886875	0.000033	0.0012	0.00000	0.04418389	0.0000948	2.777E+09	0.280986316	-0.4	0.280986	4.26047E-05	-0.4	1.5	0.280984	-0.4	3.34	3.05		3.339	3.052
MK2-13.2	0.281104	0.000011	0.008665703	0.0000114	1.467234	0.0000143	1.88686	0.000031	0.0015	0.00001	0.05592822	0.000302	2.777E+09	0.281024041	1.0										3.233	3.000
MK2-A	0.281139	0.000012	0.008660825	0.0000139	1.467289	0.0000144	1.88683	0.0000337	0.0027	0.00001	0.1009259	0.000329	2.777E+09	0.280996504	0.0										3.310	3.038
MK2-9	0.281006	0.000008	0.00865222	0.00000752	1.467252	0.0000115	1.886784	0.0000257	0.0007	0.00002	0.02671534	0.000708	2.777E+09	0.280967457	-1.1										3.392	3.078
MK2-8	0.281053	0.000010	0.00866862	0.00000967	1.467236	0.0000124	1.886837	0.0000299	0.0010	0.00002	0.03597279	0.000591	2.777E+09	0.281000987	0.1										3.298	3.032
MK2-B	0.281096	0.000012	0.008687851	0.0000127	1.46726	0.0000143	1.88686	0.0000324	0.0021	0.00002	0.08219662	0.000742	2.777E+09	0.280982523	-0.5										3.350	3.057
MK2-C	0.281002	0.000008	0.008663447	0.00000746	1.467252	0.0000111	1.886797	0.0000267	0.0007	0.00000	0.02085691	0.000155	2.777E+09	0.280966085	-1.1										3.396	3.080
MK2-D	0.281033	0.000010	0.008652979	0.0000102	1.467272	0.0000124	1.886811	0.0000266	0.0014	0.00002	0.04856023	0.00062	2.777E+09	0.280960636	-1.3										3.411	3.087
MK2-12.1	*0.281016*	*0.000009*	*0.008651225*	*0.00000936*	*1.467258*	*0.0000116*	*1.886874*	*0.0000296*	*0.0010*	*0.00001*	*0.03352143*	*0.000523*	*2.457E+09*	*0.280970727*	*-8.4*										*3.758*	*3.092*
MK2-12.2	*0.281074*	*0.000014*	*0.008626283*	*0.0000146*	*1.467277*	*0.0000175*	*1.886826*	*0.0000469*	*0.0014*	*0.00001*	*0.0510428*	*0.00046*	*2.062E+09*	*0.281018602*	*-15.9*										*4.094*	*3.048*

The measured $^{176}Hf/^{177}Hf$ ratios for the unknowns were calculated to their initial value using the measured $^{176}Lu/^{177}Hf$ ratios, an ^{176}Lu decay constant of $1.867 \cdot 10^{-11}$ year^{-1} (Scherer et al., 2007) and the emplacement ages obtained during previous studies (Table 1). The calculations of epsilon Hf were done with a present-day chondritic 176Hf/^{177}Hf value of 0.282785 and $^{176}Lu/^{177}Hf$ of 0.0336 (Bouvier et al., 2008). Depleted mantle parameters are $^{176}Hf/^{177}Hf$ 0.28325 and $^{176}Lu/^{177}Hf$ of 0.0388, following Griffin et al. (2000).
Analyses in italics excluded from average; those underlines excluded from median.
TDM2a: depleted mantle extraction age for mafic protolith
TDM2a: depleted mantle extraction age for tonalitic protolith
TDM calculated using:

$$\frac{\ln\left(\frac{\left(\left(\frac{^{176}Hf}{^{177}Hf}\right)_{DM,0}+\left(\frac{^{176}Lu}{^{177}Hf}\right)_{DM,0}-\left(\frac{^{176}Hf}{^{177}Hf}\right)_{zirc,i}-\left(\frac{^{176}Lu}{^{177}Hf}\right)_{crust,i}\right)*e^{(\lambda*agezircon)}}{\left(\left(\frac{^{176}Lu}{^{177}Hf}\right)_{DM,0}*e^{(\lambda*agezircon)}-\left(\frac{^{176}Lu}{^{177}Hf}\right)_{crust,i}\right)}\right)}{\lambda}$$

	176Hf/177Hf	SE	174Hf/177Hf	SE	178Hf/177Hf	SE	180Hf/177Hf	SE	176Lu/177Hf	SE	176Yb/177Hf	SE	AGE	INITIAL
TRA_Data_39409-MT-1.csv	0.282490	0.000005	0.008656	0.000004	1.467277	0.000009	1.886812	0.000020	0.000017	0.000000	0.000722	0.000006	732000000	0.28249
TRA_Data_39411-MT-2.csv	0.282507	0.000005	0.008671	0.000004	1.467273	0.000008	1.886830	0.000019	0.000011	0.000000	0.000450	0.000003	732000000	0.28251
TRA_Data_39437-MT-03.csv	0.282481	0.000005	0.008651	0.000004	1.467266	0.000009	1.886837	0.000020	0.000011	0.000000	0.000446	0.000003	732000000	0.28248
TRA_Data_39438-MT-04.csv	0.282494	0.000005	0.008663	0.000004	1.467272	0.000009	1.886817	0.000019	0.000028	0.000000	0.001174	0.000003	732000000	0.28249
TRA_Data_39442-MT-05.csv	0.282494	0.000005	0.008656	0.000004	1.467275	0.000009	1.886832	0.000021	0.000027	0.000000	0.001145	0.000003	732000000	0.28249
TRA_Data_39443-MT-06.csv	0.282497	0.000005	0.008670	0.000004	1.467273	0.000009	1.886822	0.000018	0.000028	0.000000	0.001182	0.000003	732000000	0.28250
TRA_Data_39463-MT-07.csv	0.282505	0.000005	0.008666	0.000004	1.467271	0.000010	1.886841	0.000021	0.000025	0.000000	0.001044	0.000003	732000000	0.28250
TRA_Data_39482-MT-08.csv	0.282488	0.000005	0.008672	0.000004	1.467263	0.000009	1.886836	0.000020	0.000035	0.000000	0.001494	0.000003	732000000	0.28249
TRA_Data_39498-MT-09.csv	0.282490	0.000005	0.008650	0.000004	1.467273	0.000009	1.886823	0.000020	0.000030	0.000000	0.001301	0.000003	732000000	0.28249
TRA_Data_39504-MT-10.csv	0.282496	0.000005	0.008668	0.000004	1.467268	0.000009	1.886839	0.000021	0.000036	0.000000	0.001582	0.000003	732000000	0.28250
TRA_Data_39506-MT-11.csv	0.282501	0.000005	0.008672	0.000004	1.467246	0.000009	1.886873	0.000018	0.000023	0.000000	0.000977	0.000003	732000000	0.28250
TRA_Data_39522-MT-12.csv	0.282510	0.000005	0.008671	0.000004	1.467248	0.000009	1.886772	0.000021	0.000032	0.000000	0.001374	0.000003	732000000	0.28251
TRA_Data_39550-MT-13.csv	0.282487	0.000005	0.008653	0.000004	1.467257	0.000009	1.886859	0.000019	0.000035	0.000000	0.001535	0.000003	732000000	0.28249
TRA_Data_39565-MT-14.csv	0.282499	0.000005	0.008661	0.000004	1.467266	0.000009	1.886839	0.000021	0.000031	0.000000	0.001318	0.000003	732000000	0.28250
TRA_Data_39585-MT-15.csv	0.282478	0.000005	0.008649	0.000004	1.467276	0.000008	1.886863	0.000018	0.000039	0.000000	0.001737	0.000003	732000000	0.28248
TRA_Data_39597-MT-16.csv	0.282497	0.000005	0.008657	0.000004	1.467245	0.000009	1.886799	0.000021	0.000028	0.000000	0.001208	0.000003	732000000	0.28250
	0.282495	0.000018												
TRA_Data_39413-LV11-1.csv	0.282807	0.000004	0.008666	0.000004	1.467282	0.000006	1.886830	0.000014	0.001226	0.000003	0.065179	0.000201	290000000	0.28280
TRA_Data_39439-LV11-02.csv	0.282815	0.000009	0.008664	0.000010	1.467282	0.000010	1.886801	0.000021	0.002678	0.000002	0.149247	0.000064	290000000	0.28280
TRA_Data_39464-LV11-03.csv	0.282810	0.000009	0.008651	0.000011	1.467235	0.000011	1.886799	0.000022	0.002607	0.000001	0.147064	0.000132	290000000	0.28280
TRA_Data_39483-LV11-04.csv	0.282825	0.000010	0.008688	0.000011	1.467303	0.000010	1.886830	0.000022	0.002911	0.000006	0.171454	0.000417	290000000	0.28281
TRA_Data_39499-LV11-05.csv	0.282814	0.000009	0.008681	0.000011	1.467278	0.000010	1.886876	0.000024	0.002975	0.000000	0.174036	0.000096	290000000	0.28280
TRA_Data_39507-LV11-06.csv	0.282812	0.000007	0.008686	0.000007	1.467274	0.000009	1.886775	0.000021	0.001691	0.000001	0.099293	0.000209	290000000	0.28280
TRA_Data_39551-LV11-07.csv	0.282825	0.000009	0.008650	0.000011	1.467296	0.000008	1.886898	0.000022	0.003909	0.000063	0.221444	0.003350	290000000	0.28280
TRA_Data_39584-LV11-08.csv	0.282803	0.000006	0.008663	0.000007	1.467246	0.000009	1.886796	0.000019	0.001726	0.000003	0.099349	0.000119	290000000	0.28279
	0.282814	0.000016												
TRA_Data_39414-TEM2-1.csv	0.282649	0.000015	0.008691	0.000013	1.467354	0.000017	1.886870	0.000038	0.001544	0.000006	0.052991	0.000074	417000000	0.28264
TRA_Data_39416-TEM2-02.csv	0.282673	0.000007	0.008647	0.000007	1.467299	0.000010	1.886780	0.000021	0.001202	0.000003	0.043976	0.000064	417000000	0.28266
TRA_Data_39440-TEM2-03.csv	0.282627	0.000009	0.008662	0.000010	1.467286	0.000012	1.886905	0.000029	0.002307	0.000017	0.069269	0.000242	417000000	0.28261
TRA_Data_39441-TEM2-04.csv	0.282649	0.000009	0.008651	0.000009	1.467310	0.000012	1.886880	0.000029	0.001418	0.000007	0.044299	0.000080	417000000	0.28264
TRA_Data_39465-TEM2-05.csv	0.282679	0.000008	0.008666	0.000009	1.467279	0.000011	1.886881	0.000025	0.001393	0.000008	0.050914	0.000291	417000000	0.28267
TRA_Data_39484-TEM2-06.csv	0.282664	0.000009	0.008667	0.000010	1.467304	0.000012	1.886920	0.000026	0.002040	0.000006	0.072926	0.000186	417000000	0.28265
TRA_Data_39497-TEM2-07.csv	0.282685	0.000010	0.008647	0.000009	1.467282	0.000013	1.886838	0.000027	0.001963	0.000043	0.070869	0.001300	417000000	0.28267
TRA_Data_39508-TEM2-08.csv	0.282654	0.000008	0.008659	0.000009	1.46728	0.000011	1.886832	0.000024	0.001756	0.000003	0.064344	0.000096	417000000	0.28264
TRA_Data_39535-TEM2-09.csv	0.282635	0.000010	0.008653	0.000010	1.467311	0.000012	1.886936	0.000028	0.001268	0.000020	0.045844	0.000580	417000000	0.28263
TRA_Data_39536-TEM2-10.csv	0.282646	0.000008	0.008669	0.000009	1.467322	0.000012	1.886912	0.000026	0.001513	0.000003	0.055614	0.000132	417000000	0.28263
TRA_Data_39539-TEM2-11.csv	0.282662	0.000009	0.008683	0.000010	1.467264	0.000012	1.886867	0.000026	0.002216	0.000010	0.080522	0.000312	417000000	0.28264
TRA_Data_39564-TEM2-12.csv	0.282671	0.000007	0.008670	0.000008	1.467255	0.000011	1.886878	0.000025	0.000985	0.000004	0.034351	0.000136	417000000	0.28266
TRA_Data_39598-TEM2-13.csv	0.282662	0.000007	0.008686	0.000008	1.467278	0.000010	1.886817	0.000023	0.001383	0.000005	0.047327	0.000088	417000000	0.28265
	0.282658	0.000034												

Data for figure 3:

Cornell, D.H., Minnaar, H., Frei, D. and Kristoffersen, M., 2018. Precise microbeam dating defines three Archaean granitoid suites at the southwestern margin of the Kaapvaal Craton. Precambrian Research, 304, 21-38.
Frimmel, H.E., Zeh, A., Lehrmann, B., Hallbauer, D. and Frank, W., 2009. Geochemical and Geochronological Constraints on the Nature of the Immediate Basement next to the Mesoarchaean Auriferous Witwatersrand Basin, South Africa. Journal of Petrology, 50, 2187-2220.
Hicks, N., Elburg, M. and Andersen, T., 2015. U-Pb and Hf isotope constraints for emplacement of the Nkandla Granite, Southeastern Kaapvaal Craton, South Africa. South African Journal of Geology, 118, 119-128.
Laurent, O. and Zeh, A., 2015. A linear Hf isotope-age array despite different granitoid sources and complex Archean geodynamics: Example from the Pietersburg block (South Africa). Earth and Planetary Science Letters, 430, 326-338.
Magwaza, B.N., 2020. Isotopic resetting of zircon: Influence of age, temperature and chemical environment, Department of Geology. University of Johannesburg, Johannesburg.
Murphy, R.C.L., 2015. Stabilising a Craton: the Origin and Emplacement of the 3.1 Ga Mpuluzi Batholith. PhD thesis, Macquarie University, Sydney.
Reinhardt, J., Elburg, M.A. and Andersen, T., 2015. Zircon U-Pb age data and Hf isotopic signature of Kaapvaal Basement granitoids from the Archaean White Mfolozi Inlier, Northern Kwazulu-Natal. South African Journal of Geology, 118, 473-488.
Vezinet, A., 2017. Differentiation and stabilisation of the Archaean continental crust, the example of the northern edge of the Kaapvaal Craton, South Africa, Department of Geology. PhD thesis, University of Stellenbosch and Université Jean Monnet, p. 334.
Zeh, A., Gerdes, A. and Barton, J.M., 2009. Archean Accretion and Crustal Evolution of the Kalahari Craton-the Zircon Age and Hf Isotope Record of Granitic Rocks from Barberton/Swaziland to the Francistown Arc. Journal of Petrology, 50, 933-966.
Zeh, A., Gerdes, A. and Millonig, L., 2011. Hafnium isotope record of the Ancient Gneiss Complex, Swaziland, southern Africa: evidence for Archaean crust-mantle formation and crust reworking between 3.66 and 2.73 Ga. Journal of the Geological Society, 168, 953-963.
Zeh, A., Jaguin, J., Poujol, M., Boulvais, P., Block, S. and Paquette, J.-L., 2013. Juvenile crust formation in the northeastern Kaapvaal Craton at 2.97Ga—Implications for Archean terrane accretion, and the source of the Pietersburg gold. Precambrian Research, 233, 20-43.

Additional data figure 4:

Andersen, T., Elburg, M.A. and Van Niekerk, H.S., 2019. Detrital zircon in sandstones from the Palaeoproterozoic Waterberg and Nylstroom basins, South Africa: Provenance and recycling. South African Journal of Geology, 122, 79-96.
Koglin, N., Zeh, A., Frimmel, H.E. and Gerdes, A., 2010. New constraints on the auriferous Witwatersrand sediment provenance from combined detrital zircon U–Pb and Lu–Hf isotope data for the Eldorado Reef (Central Rand Group, South Africa). Precambrian Research, 183, 817-824.
Taylor, J., Zeh, A. and Gerdes, A., 2016. U–Pb–Hf isotope systematics of detrital zircons in high-grade paragneisses of the Ancient Gneiss Complex, Swaziland: Evidence for two periods of juvenile crust formation, Paleo- and Mesoarchaean

sediment deposition, and 3.23 Ga terrane accretion. Precambrian Research, 280, 205-220.
van Schijndel, V., Stevens, G., Zeh, A., Frei, D. and Lana, C., 2017. Zircon geochronology and Hf isotopes of the Dwalile Supracrustal Suite, Ancient Gneiss Complex, Swaziland: Insights into the diversity of Palaeoarchaean source rocks, depositional and metamorphic ages. Precambrian Research, 295, 48-66.
Wilson, A.H. and Zeh, A., 2018. U-Pb and Hf isotopes of detrital zircons from the Pongola Supergroup: Constraints on deposition ages, provenance and Archean evolution of the Kaapvaal craton. Precambrian Research, 305, 177-196.
Zeh, A. and Gerdes, A., 2012. U–Pb and Hf isotope record of detrital zircons from gold-bearing sediments of the Pietersburg Greenstone Belt (South Africa)—Is there a common provenance with the Witwatersrand Basin? Precambrian Research, 204-205, 46-56.
Zeh, A., Gerdes, A. and Heubeck, C., 2013. U−Pb and Hf isotope data of detrital zircons from the Barberton Greenstone Belt: constraints on provenance and Archaean crustal evolution. Journal of the Geological Society, 170.
Zeh, A., Wilson, A.H. and Ovtcharova, M., 2016. Source and age of upper Transvaal Supergroup, South Africa: Age-Hf isotope record of zircons in Magaliesberg quartzite and Dullstroom lava, and implications for Paleoproterozoic (2.5–2.0 Ga) continent reconstruction. Precambrian Research, 278, 1-21.